

Generation of Magnetic Fields in Plasmas

Nitin Shukla



Department of Physics
Umeå 2012

Copyright© Nitin Shukla
ISBN: 978-91-7459-394-5.
Elektronisk version tillgänglig på <http://umu.diva-portal.org/>
Tryck/Printed by: Print & Media
Umeå, Sweden 2012

*To my parents Late Shree Prabha Shankar Shukla and my loving mother
Kaminee Shukla for their blessings, inspiration and for their constant
supporting of my dreams.*

Abstract

Relativistic and non-relativistic plasma outflows are quite ubiquitous in astrophysical scenarios, as well as in laboratory plasmas. The propagation of relativistic and non-relativistic charged particle beams in background plasmas provides return currents in the opposite direction and interactions between the currents then drive several plasma instabilities involving the longitudinal (electrostatic instabilities) and transverse (electromagnetic instability) modes. Such instabilities have been accepted as possible mechanisms for generating spontaneous magnetic fields in extreme astrophysical environments, such as the gamma-ray bursts (GRBs), pulsar magnetosphere, active galactic nuclei (AGN), as well as in laboratory plasmas such as those in inertial confinement fusion schemes.

In the present thesis, we have studied several aspects of waves and instabilities in both unmagnetized and magnetized plasmas. We have calculated the linear growth rates of the plasma instabilities that can occur in the presence of counter-propagating anisotropic plasmas (the Weibel instability/filamentation instability) in an unmagnetized plasma, due to the counter-streaming of electrons and positrons in uniform and nonuniform magnetoplasmas, and by a nonstationary ponderomotive force of an electromagnetic wave in a warm plasma.

Comprehensive analytical and numerical studies of plasma instabilities have been made to understand possible mechanisms for purely growing magnetic fields in the presence of mobile/immobile ions and (or) cold/mildly hot electron beams. The theory has been developed for a proper understanding of fast as well as slow phenomena in plasmas by using the kinetic, fluid and magnetohydrodynamic (MHD) approaches. Specific applications are presented, including inertial confinement fusion; Gamma-rays bursts (GRBs), and pulsar magnetosphere.

We have also studied new and purely growing modes in quantum-plasmas, which happen to be a rapidly growing emerging subfield of plasma physics. We have investigated an oscillatory instability involving dust acoustic-like waves due to a relative drift between the ions and the charged dust particles in quantum dusty magneto-plasma. This study can be of importance in semiconductor plasmas or in astrophysical plasmas, such as those in the cores of white dwarfs.

Sammanfattning

Relativistiska och icke-relativistiska partikelflöden är vanliga inom astrofysikaliska scenarier lika väl som i laboratorieplasmor. Utbredningen av relativistiska och icke-relativistiska laddade partikel-strålar i bakgrundsplasmata genererar strömmar i den motsatta riktningen, och växelverkan mellan dessa strömmar kan sedan driva olika sorters plasma instabiliteter, inklusive longitudinella (elektrostatiskt instabila) och transversella (elektromagnetiskt instabila) moder. Sådana instabiliteter har lagts fram som möjliga mekanismer för spontan generering av magnetfält i astrofysikaliska miljöer, såsom gammablixtar (GRB), pulsar magnetosfärer, aktiva galaxkärnor, lika väl som i laboratorie-plasmor, exempelvis i samband med tröghetsfusion.

I denna avhandling har flera aspekter av vågor studerats, både i magnetiserade och omagnetiserade plasmor. Den linjära tillväxthastigheten har beräknats för mot-strömmande anisotropa plasmor (Weibel-instabilitet/Filamentations instabilitet) i ett icke-magnetiserat plasma, p. g. a. driften mellan elektroner och positroner i homogena såväl som inhomogena plasmor, samt p. g. a. den ponderomotiva kraften från en elektromagnetisk våg i ett varmt plasma.

Omfattande analytiska och numeriska studier av plasma instabiliteter har gjorts för att förstå möjliga mekanismer för magnetfältsförstärkning i närvaro av rörliga/orörliga joner och/eller kalla/varma elektronstrålar. Teorin har utvecklats för att nå en djupare förståelse av snabba såväl som långsamma fenomen i plasmor genom användande av kinetiska modeller, vätskemodeller och magnetohydrodynamiska (MHD) modeller.

Specifika tillämpningar presenteras mot tröghetsfusion, gammablixtar and pulsar magnetosfärer. Tillväxten hos nya vågmoder i kvantplasmor studeras också, vilket är ett nytt snabbt växande delområde av plasmafysiken. Slutligen studeras en oscillerande instabilitet hos damm-akustiska vågor orsakad av en drift mellan joner och laddade damm-partiklar i ett kvantplasma. Denna studie kan vara av betydelse för halvledar-plasmor och astrofysikaliska plasmor, exempelvis i de centrala delarna av en vit dvärg.

LIST OF PUBLICATIONS

The thesis is based on the following papers:

1. *Nitin Shukla & P. K. Shukla*, Generation of magnetic field fluctuations in relativistic electron-positron magnetoplasmas , *Phys. Lett. A*, **362**, 221-224 (2007).
2. *Nitin Shukla & P. K. Shukla*, A new purely growing instability in a strongly magnetized nonuniform pair plasma, *Phys. Lett. A* **367**, 120-122, (2007).
3. *N. Shukla, P. K. Shukla & G. E. Morfill*, Amplification of magnetic fields by polaritonic flows in quantum pair plasmas. *J. Plasma Phys.* **73**, 289-293, (2007).
4. *Nitin Shukla, P. K. Shukla, G. Brodin & L. Stenflo*, Ion streaming instability in a quantum dusty magnetoplasma, *Phys. Plasmas* **15**, 044503 (2008).
5. *Nitin Shukla, P. K. Shukla, & L. Stenflo*, Magnetization of a warm plasma by the non-stationary ponderomotive force of an electromagnetic wave, *Phys. Rev. E* **80**, 027401, (2009).
6. *Nitin Shukla & P. K. Shukla*, Proton-temperature anisotropy driven magnetic fields in plasmas with cold and relativistically hot electrons, *J. Plasma Phys.* **76**, 1-5 (2010).
7. *Nitin Shukla, A. Stockem, F. Fiúza & L. O. Silva*, Enhancement in the electromagnetic beam-plasma instability due to ion streaming, *J. Plasma Phys.* **78**, 181-187 (2012). endenumerate

Contents

1	Introduction	1
1.1	Motivation and background	1
1.2	Outline of the Thesis	9
2	Properties of plasmas	10
2.1	Basics of plasma physics	10
2.2	Criteria for the plasma state	12
2.3	Physical regimes for classical and quantum plasmas	12
2.4	Basic parameters for quantum plasmas	13
2.5	Quantum dusty plasmas	14
2.6	Theoretical descriptions of plasmas	14
2.6.1	Single particle motion	15
2.6.2	Kinetic Model	17
2.6.3	The fluid model	18
2.6.4	The MHD model	20
2.7	Conclusion	24
3	Waves in plasmas	25
3.1	Waves in an unmagnetized plasma	25
3.1.1	Electrostatic electron plasma (ESEP) waves in an unmagnetized plasma	26
3.1.2	Electromagnetic (EM) waves in an unmagnetized plasma	29
3.2	Waves in magnetized plasma	30
3.3	Summary	32
4	Mechanisms for the plasma magnetization	34
4.1	Motivation	34
4.2	The $\nabla n_e \times \nabla T_e$ (The Biermann battery)	35
4.3	The Weibel instability	37
4.4	Plasma magnetization by a nonuniform electromagnetic beam	40
4.5	Summary and conclusion	43
5	Summaries of the papers	44
	Bibliography	49

Introduction

1.1 Motivation and background

Understanding the origin of magnetic fields in cosmic and laser produced plasmas has been of great theoretical as well as experimental interest [1–3]. The generation of seed magnetic fields in the early universe is a long-standing mystery in astrophysics. A very weak magnetic field (typically of the order of one to thirty microgauss) in the early universe has been of much interest to the scientific community. Our galaxy and many other spiral galaxies are endowed with coherent magnetic fields ordered on scales ≈ 10 kpc with typical strength $B_G = 3 \times 10^{-6}$ G [4, 5]. Furthermore, the cosmic magnetic field is strongly correlated with the large-scale structures (e.g. currents filaments and sheets) of the Universe [6, 7]. The origin of cosmological, galactic and large-scale extra-galactic magnetic fields is one of the main unresolved problems of astrophysics and cosmology.

The existence of these magnetic fields are relevant to the processes which took place in the early universe. Because of the Universe's high conductivity, two important quantities are almost conserved during the evolution of the Universe: the magnetic flux and the magnetic helicity. The magnetic field in ionized media is generated on account of electrical currents or of rotational electric fields. The self-excitation of large scale magnetic fields B in astrophysical bodies, such as the Sun, stars, galaxies, etc [8, 9], is a challenging issue. The main problem of most particle physics mechanisms of the origin of seed magnetic fields is how to produce them coherently on cosmological (large) scales [10].

The production of large quasi-static magnetic fields has been observed in Laser-produced plasma. In early experiments [11] it was observed that such magnetic fields can exceed 100-200 kG in underdense plasma $n_e \simeq 0.2n_c$, where n_c is the critical density. This experiment used a Nd-glass laser producing a short pulse less than 100 ps aimed at a target larger than $100 \mu m$ in diameter. For laser pulse lengths longer than 1 ns, one obtains a larger-scale toroidal magnetic field surrounding the laser spot. One is then tempted to attribute these toroidal fields to the $\nabla n \times \nabla T$ mechanism [12]. The Faraday rotation of a high frequency electromagnetic probe beam has been used to

detect such magnetic fields [13].

The recent developments of ultra-intense laser beams (intensity of the order of $10^{21} - 10^{22} \text{ W/cm}^2$) with durations shorter than 1 picosecond (ps), open new possibilities to implement different mechanisms for magnetic field generation that can be significant in inertial confinement fusion (ICF) experiments [14, 15]. In this approach, a small spherical pellet containing micrograms of deuterium-tritium (DT) is compressed by powerful laser beams. The enormous energy influx explodes the outer layer of the target; the remaining portion of the target is then driven inward. As a result, a shock wave forms which is hot and dense enough to ignite the DT fuel [16]. Two approaches have been systematically investigated; direct drive and indirect drive. In the indirect drive the laser energy is converted into x-rays by the interaction of the hohlraum [17], to obtain a symmetric compression from a limited amount of laser beam lines, whereas in the direct drive scheme a large number of beam lines is used to directly obtain a symmetric compression directly from the laser light [18].

The fast ignition scheme (FIS) is a more recent and alternative approach for ICF. The advantage of this scheme is that it is very efficient in terms of lower driver and higher gain energy. It is also economically less expensive than conventional inertial confinement fusion. The scheme of FI by an ultra-intense laser beam [19] is illustrated in figure 1.1. In this scheme, a capsule of DT fuel is implanted on a gold cone. The spherical pellet of DT is compressed having a density in the core of a target of the order of 300g/cm^3 . Then, a very-short ($\sim 10\text{ps}$) ultra-high-power ($\sim 70\text{KJ}, 4\text{PW}$) intense laser beam is injected onto the gold cone. When this pulse interacts with the fuel, it produces highly energetic (3.5MeV) relativistic electrons. These electron beams transport the energy to ignite the hot spot in the core of the pre-compressed target and heat up the fuel to 100 million degrees centigrade, which is hot enough for thermonuclear reactions [20, 21].

The propagation of a short laser pulse in an overdense plasma has been widely examined [22]. It was found that high intensity laser pulses drive the electrons in the forward direction. For such highly intense laser pulses, the electron quiver velocity becomes relativistic and with its progress in the background plasma, a return electron current flows in the opposite direction to maintain the global charge neutrality. This implies unstable modes of the two counterpropagating beams which produces anisotropy in the plasma temperature and eventually leads to the Weibel instability driven by anisotropic velocity distributions. The collisionless Weibel instability also appears in the coronal region, typically for densities below 10^{24}cm^{-3} [23]. The evolution of the instability can be divided into two stages. In the linear stage, the fast MeV-beam electrons move into the target; initially, the plasma electrons respond to

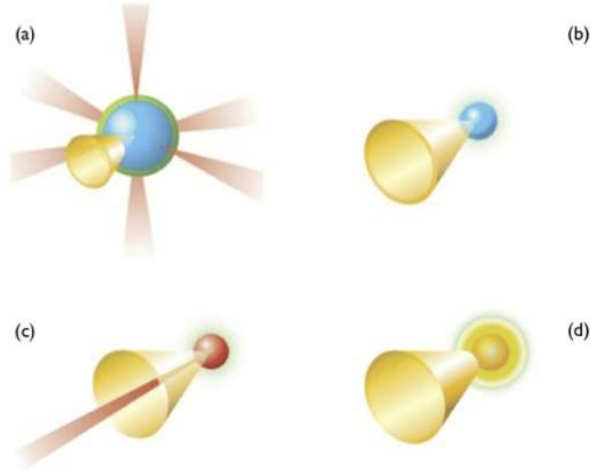


Figure 1.1: The standard scheme of Fast Ignition (FI): (a) capsule of DT fuel with an imbedded cone of gold is irradiated by many symmetrically arranged laser beams, (b) the material converges around the tip of a gold cone. The density of the DT is now hundreds of times the density of solid material, (c) An ultra intense laser is fired onto the gold cone. When the laser beam interacts with the tip of the gold cone, a large number of energetic electrons are produced, (d) The energetic electrons travel into the dense DT fuel and deposit their energy. This raises the fuel to 100 million degrees centigrade, which is hot enough to initiate the fusion reactions. (Courtesy of HiPER)

the instability and a return current is set up compensating the micro-currents carried by the fast MeV-beam electrons. These currents induce the magnetic field that reinforces the initial disturbance. This instability generates electromagnetic fields, creating current filaments and the magnetic field amplification. It is found that the instability grows with $\Gamma \sim \omega_{pe0}^{-1}$ in the linear stage [24]. Later the magnetic field decays rapidly due to the fact that the electrons reach thermal equilibrium and the ions begin to respond to the instability. As a result, the Weibel instability ceases at $100\omega_{pe0}^{-1}$. The Weibel instability breaks the flow of particles into tiny dissipated magnetic fields and can be susceptible to the energy deposition in the core of the compressed fusion pellet. At this stage, the linear instability enters into the nonlinear dissipative stage and the gets filamented. Theoretically, it has been predicted that the magnetic field saturates at $B_{sat} \propto \Gamma^2$ [25] and reaches a quasi-steady linear level with no or very slow decay on a time scale much longer than $100\omega_{pe0}^{-1}$. One of the obstacles in this scheme is to deposit $10keV$ energy in a small region of radius $20 \mu m$ near the compressed target core due to plasma instabilities. Both the analytical and numerical simulations reveal that these instabilities can play an important role in stopping the hot electrons in the core [26, 27]. One of the key issues in the FIS is the deposition of the beam energy in

the plasma core, which is required to ignite fusion. Actually, spontaneously generated magnetic fields by these plasma instabilities are an undesirable effect in FIS scenarios [28]. Hence, in order to design the FI experiment, it is necessary to understand the consequence of the instabilities. This will help to improve the FI design. Several experiments have been conducted to inspect the role of the Weibel instability in different scenarios [29, 30].

In many previous works, the linear and nonlinear stages of the Weibel instability have been investigated theoretically and numerically by assuming immobile ions, which form a neutralizing background, because their impact is visible on longer time scales only. Thus, the role of ions is relatively unexplored yet, but necessary for the treatment of realistic scenarios and the large time scales of the shock formation process [31]. The question arises whether the inclusion of the ion dynamics still drives the electromagnetic or the Weibel-type instability on the ion time scale after the electron Weibel instability has saturated. At this stage, the electron temperature is quite high but the evolution of ions is slow due to their inertia, and thus the ion temperature of the ions T_i is still different from T_e . With this in mind in paper VII, we investigated the Weibel instability in a counter-propagating electron-ion plasma with the focus on contribution due to a realistic mass ratio. Furthermore, in paper VI, we demonstrated the role of purely growing electromagnetic instabilities driven by anisotropic protons in the presence of cold and relativistically hot electrons in plasmas. Magnetic fields can also be generated by the interaction of an intense laser pulse with a solid density plasma target. The non-stationary ponderomotive force of a large-amplitude electromagnetic wave pushes the electrons in the propagation direction, thus generating a temperature anisotropy and the magnetic fields, which have been investigated in paper V.

The importance of large-scale magnetic fields has also been recognized in a number of astrophysical sources, such as the gamma-ray bursts [32] and relativistic jets [33]. In fact, great efforts have been made to understand the cause of these magnetic fields. But the source of these strong magnetic fields is still not understood and remains a mysterious question. These seed magnetic fields are required for nonthermal radiation and particle acceleration in astrophysics. Moreover, the plasma instabilities are proposed as the first stage of suitable mechanism generating strong magnetic fields. Such plasma instabilities are ubiquitous in astrophysical scenarios. In other words, the natural occurrence of these plasma instabilities may generate strong magnetic fields, which are required for nonthermal radiation in GRBs. The dynamics of relativistic outflows appears to be an important research field to study. The importance of collisionless plasma dynamics and plasma instabilities has been studied in

connection with many outstanding problems in astrophysics [34]. One of the general consensuses in the scientific community is that the plasma instabilities are plausible mechanisms for the magnetic field generation in astrophysics, especially in Gamma-Ray Bursts (GRBs). In this section, we will briefly introduce the phenomenon of GRBs and then discuss the role of the electromagnetic beam-plasma instability (the Weibel instability), which plays a role in GRBs.

The Gamma-ray bursts (GRBs) are intense flashes of gamma-radiation that can last from milliseconds to several minutes (figure 1.2). The GRBs were first discovered in 1967 by the Vela satellites [35]. The GRBs are believed to be caused by very energetic explosions, when a large amount of energy $E \sim 10^{51} - 10^{53} \text{erg}$ is released over a few seconds in a small volume [36]. The GRBs are luminous electromagnetic events produced in so called fireballs. Such fireballs consist primarily of electron-positron pairs together with a small amount of baryonic mass, $M \ll E/c^2$. There seem to be two kind of GRBs, long bursts that last longer than a few seconds typically $T > 2s$, and short ones that last less than a few seconds, $T < 2s$. The emitted jets of high-energy particles move with relativistic velocities of $\gamma \sim 10^2 - 10^3$ (γ is the Lorentz factor). Most observed GRBs are believed to be narrow beams of intense radiation. The interaction of these energetic particles with the ambient medium produces light at all wavelengths from γ -rays to radio waves and ultra-relativistic energy flows are converted to radiation. It was found that the main radiation process involved in the GRBs scenarios is synchrotron radiation [37, 38], which is determined by the magnetic field strength. The detected radiation allows for the measurement of the magnetic field strength, which can be compared with theoretical models and simulations. On large scales, the interaction of particle jets with a pre-existing plasma can lead to the formation of shocks, where the magnetic field was observed to be amplified substantially at the shock front. Often, an electromagnetic wave propagating ahead of the shock is present, the so-called precursor. The large size of the shock provides enough time for plasma instabilities to occur between the precursor and the surrounding medium. Here, we do not provide a fully consistent theory of the shock model, but focus on the precursor regime and the generation of plasma instabilities and the self-consistently generated magnetic fields.

Several mechanisms have been proposed to explain the generation of seed magnetic fields in GRBs. But most of the mechanisms failed to explain the required equipartition of magnetic fields generated in GRBs, since the magnetic fields turn out to be too weak. Medvedev and Loeb [39] studied the equipartition of magnetic fields that involve a relativistic two-stream (Weibel) instability in an astrophysical scenario. It was noted that the Weibel instability plays a crucial role in generating relatively strong

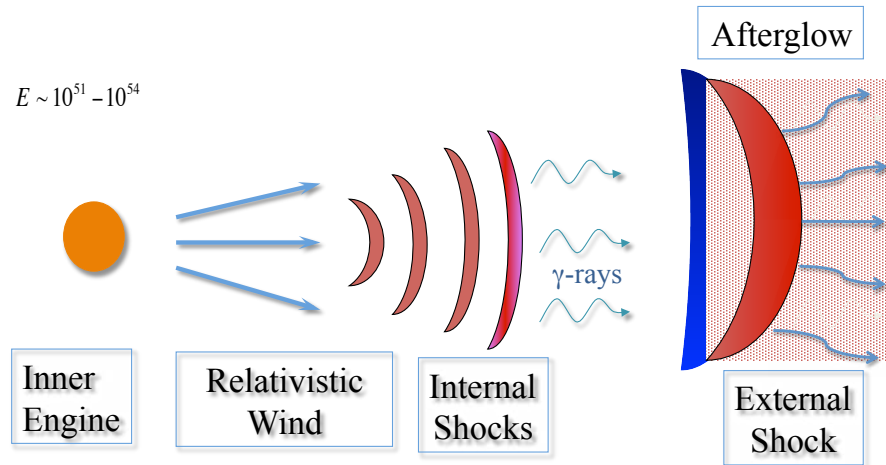


Figure 1.2: *Cartoon of a fireball*

magnetic fields. The mechanism can be described in the following way in connection with GRBs; When the GRB explodes, it ejects out a dense relativistic jet which collides with interstellar plasmas. Thus, a counter-streaming profile forms and the instability can arise. In general, longitudinal and transverse instabilities occur simultaneously. Theoretical studies have been made to understand and to explain the fastest growing instability which can generate strong magnetic fields [40]. It is found that only purely transverse electromagnetic instabilities can generate strong magnetic fields, which can then scatter charged particles that emit the electromagnetic radiation. The result of numerical simulations confirms the validity of the above mechanism in astrophysical scenarios. Many 2D and 3D numerical simulations have been performed by colliding two plasma shells [41, 42]. Simulation results show that these plasma instabilities cause the rapid growth of the magnetic fields. When the latter are strong enough, charged particles are trapped in the magnetic field. This magnetic field merges into the filaments causing the magnetic energy to cascade from the initial skin depth scale c/ω_{pe} to larger scales. Later, it is saturated at a time scale of the order $100 \omega_{pe0}^{-1}$, achieving a near equipartition field. The magnetic field energy density is then comparable with the initial particle energy density. The ratio between the energy density in the B-field and the initial kinetic energy density is of the order of $10^{-3} - 10^{-5}$ [43]. In the case of a pure electron-positron plasma, computer simulations have conclusively demonstrated that the generated magnetic field reaches sub-equipartition and grows to about 10% of the initial kinetic energy density [44]. The obtained values of the equipartition parameter 10^{-2} agree with the values inferred from GRB afterglows [45]. It is concluded that this instability can be the main mechanism to generate the sub-equipartition magnetic fields required to explain the afterglow emission of GRBs.

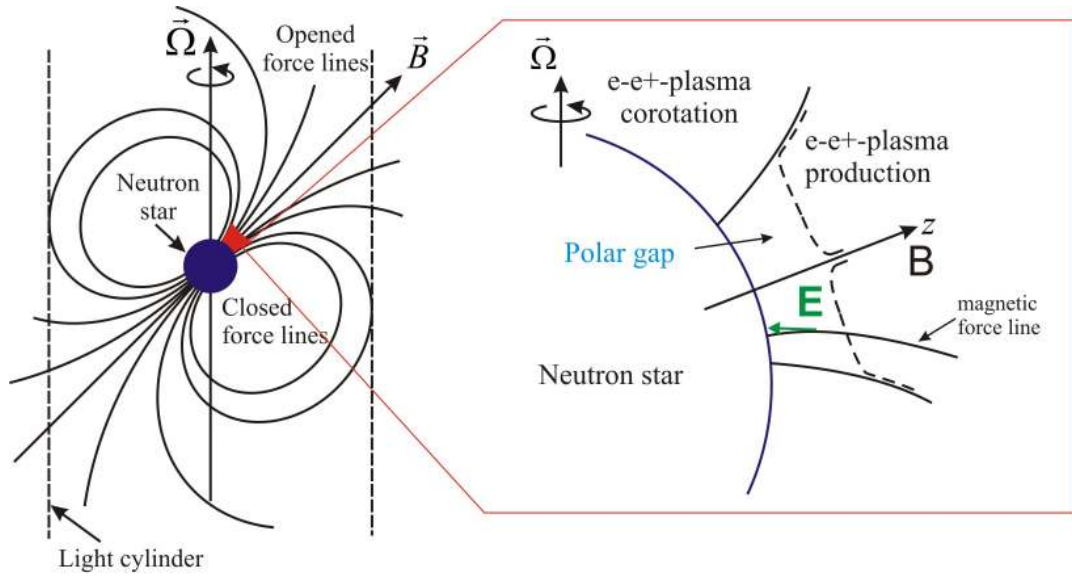


Figure 1.3: *Carton of a Pulsar: Credit: <http://science.nasa.gov/science-news>*

Many exotic astrophysical environments, such as pulsars, are embedded in strong magnetic fields ($B \sim 10^{12} - 10^{13}$ G) 1.3. In 1967, J. Bell and A. Hewish discovered the emission of a highly stable train of radio pulses [46, 47]. Due to the stability of the pulse period, Thomas Gold concluded that pulsars must be highly magnetized. Pulsars are rapidly rotating, strongly magnetized neutron stars that emit radio waves. A huge potential difference is generated between different parts of a rotating magnetized neutron star, which causes a coherent process to produce the pair plasma in the pulsar magnetosphere. In the polar-cap region, such outflows produce intense radiation, as seen in the electromagnetic spectrum. A single-particle approach has been introduced to describe possible radiation sources, but it fails to explain the highest energy observed [48]. It is these bunched particles with $\gamma_{\mp} \sim 10^3$ that would give coherent radiation in the radio range. But the growth rate of the instability is too low to account for the high level of observed radio emission.

In 1977 Cheng and Ruderman proposed a possible new mechanism where electrons and positrons of the relativistic plasma, moving along the curved open field lines of the rotating pulsar magnetosphere, would produce a net charge density and a relative streaming between the electrons and positrons [49]. As a result of the relative streaming of the plasma particles, there would appear a two-stream instability with a sufficient growth rate. This instability would be responsible for both plasma wave excitation and a bunching of charged particles. The wave vectors of unstable waves can form a wide range of angles relative to the flow velocity vector v_{\parallel} , as has been discussed for electron-positron flows [50]. Electrostatic beam-plasma instabili-

ties in the pulsar plasma are generally weaker than electromagnetic instabilities. The energy stored in the bulk motion of the plasma then converts the plasma kinetic energy into the internal energy of the radiating electrons and magnetic fields. Hence, it is important to know the description of mechanisms which helps to understand the radio emission processes in pulsar magnetospheres, radio emission from relativistic jets and relativistic expansion of strongly magnetized pair plasmas involved in the gamma-ray burst models. There has been many works in this direction [51]. The counter-streaming instability has been extensively investigated in the presence of a weak external magnetic field. In paper I, we have investigated the generation of magnetic fluctuations by field-aligned flows in plasmas. Our results show a new range of instabilities relevant to strongly flowing constant density plasmas.

Interesting results have, however, been found for the high-frequency radiation. But very few pulsars radiating with sufficiently high intensity in that frequency region have been observed. The low-frequency part of the spectrum can provide an explanation for the high effective radio temperatures of the pulsars. The low frequencies form in the inner magnetosphere, where the infinite magnetic field approximation is appropriate. Furthermore, a new purely growing instability in a strongly magnetized nonuniform pair plasma has been studied in paper II. The applications are relevant to space and tokamak plasmas.

Understanding the origin of magnetic fields in white dwarf stars and in high energy density compressed plasmas created by intense laser beams is of fundamental importance with regard to the transport of degenerate electrons in both astrophysical and inertial confinement settings. To extend our studies, we have investigated amplification of magnetic fields by polaritonic flows in quantum pair plasmas in paper III. Further, we have investigated the low-frequency waves in a quantum dusty magnetoplasma in paper VI. Such kind of plasmas are ubiquitous in compact astrophysical bodies (e.g. the interiors of white dwarf stars, magnetars and supernovae), as well as in micro- and nanoscale objects (e.g. nanowires, ultra-small semiconductor devices), which have a very high electron number density. A quantum dusty plasma consists of the electrons, ions and negatively/positively charged dust particles. Since the electrons are the lightest particles compared to the ions and charged dust particles the quantum behavior of the electrons is reached faster. In our paper, we have investigated the ion streaming instability in a quantum dusty magnetoplasma. This instability can produce a quantum dust acoustic-like wave. The result may explain the origin of the low-frequency electrostatic fluctuations in semiconductors quantum wells.

1.2 Outline of the Thesis

The aim of this doctoral thesis is to demonstrate the role of purely growing electromagnetic instabilities as one of the possible mechanisms for generating magnetic fields in uniform and nonuniform plasmas.

The thesis is organized in the following fashion. In Chapter 2, we briefly explain the underlying physics and the plasma models that we use. After the basic description of plasmas, we begin with a short introduction of waves in plasmas. Chapter 3 provides a comprehensive study of fundamental plasma wave instabilities. The approaches of several plasma wave instabilities have been provided, pointing out some of the relevant mechanism, which are of great importance for generating seed magnetic fields in plasmas. In particular, instabilities have been studied within the framework of the linear approximation.

Comprehensive and substantial concepts of waves and instabilities in plasmas are described in many textbooks. The reader is referred to e.g. *Nicholson (1983)*, *Chen (1984)*, *Lectures notes of I. H. Hutchinson(2001)*. Finally, In Chapter 5 we summarize the novel results of the papers that have been published during the course of my doctoral thesis work. The study of linear plasma wave instabilities in collisionless, homogeneous, unmagnetized electron-proton plasmas with temperature anisotropies has been performed and discussed in Papers I-VII.

Properties of plasmas

In this chapter, we describe the basic concepts, fundamental properties and criteria of plasmas. Three different approaches are briefly elaborated, in order to describe the dynamics of plasmas in electromagnetic fields.

2.1 Basics of plasma physics

Plasmas, often known as the fourth state of matter, are collections of charged particles, which exhibit quasi-neutrality and collective interactions. The term quasi-neutrality implies that the electron and ion number densities are approximately equal, viz. $n_{e0} = n_{i0}$. The concept of collective behavior implies the existence of long range electromagnetic forces (EMF) arising due to interactions between an ensemble of charged particles in plasmas. At a microscopic level, corresponding to distances shorter than the Debye radius (to be defined below), the plasma particles do not exhibit collective behavior, but instead react individually to a disturbance, for example, an electric field.

The orbit of a charged particle is controlled by the electric and magnetic fields in plasmas. However, particle motion in given fields typically gives rise to a charge imbalance. The typical length beyond which the quasi-neutrality condition can exist is represented by the Debye radius (λ_D). The potential drops exponentially with distance to any test charge particle, see fig.2.2. This phenomena is known as the Debye shielding or the screening effect in plasmas [52]. A plasma is a conductor of electricity, and a volume with dimensions greater than the Debye radius would exhibit electrically neutral behavior.

Let us suppose that a positive test charge q_t is placed inside the plasma at $\mathbf{r} = 0$. The test charge attracts all the negative charge and repels the positive charge. The charge density of the electron will increase near the test charge, while the ion number density will decrease. Hence, it will modify the charge density distribution around a test charge. The electric potential ϕ around a test particle is determined from Poisson's equation

$$\nabla^2\phi(r) = \frac{e}{\epsilon_0}[n_e(r) - n_i(r)] - \frac{q_t}{\epsilon_0}\delta(\mathbf{r} - \mathbf{v}_0t), \quad (2.1)$$

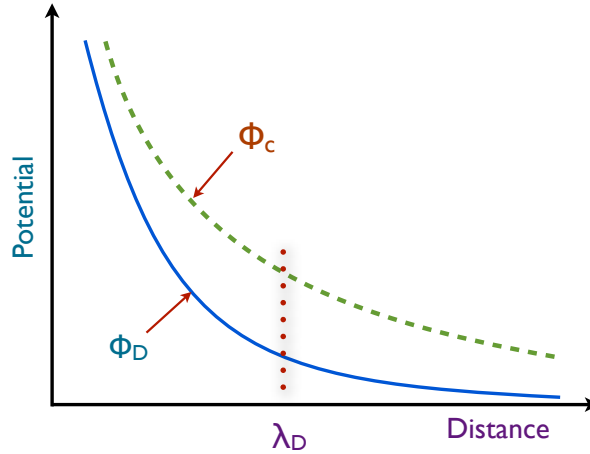


Figure 2.1: Comparison of the Debye and Coulomb potentials.

where e is the magnitude of the electron charge, ϵ_0 the permittivity of the free space, n_e, n_i are the electron and ion number densities, respectively, $\delta(\mathbf{r} - \mathbf{v}_0)$ the Dirac delta function, and \mathbf{v}_0 a constant velocity of a test charge if it moves. For a stationary test charge, we can set \mathbf{v}_0 to zero.

Now let us consider the case where a stationary test ion charge is shielded by electrons which follow the Boltzmann law, namely,

$$n_e = n_{e0} \exp\left(\frac{e\phi}{k_B T_e}\right), \quad (2.2)$$

where n_{e0} is the equilibrium electron number density, k_B the Boltzmann constant, and T_e the electron temperature. Far from origin, we have $e\phi/k_B T_e \ll 1$. Thus, the Fourier transformation of Poisson's equation yields

$$\phi(r) = \frac{qt}{8\pi^3 \epsilon_0} \int d\mathbf{k} \frac{\exp(i\mathbf{k} \cdot \mathbf{r})}{k^2 D}, \quad (2.3)$$

where we have denoted $D = 1 + 1/k^2 \lambda_{De}^2$, with the electron Debye radius given by

$$\lambda_{De} = \left(\frac{\epsilon_0 k_B T_e}{n_{e0} e^2}\right)^{1/2}. \quad (2.4)$$

The potential distribution around a test stationary ion is then the shielded Coulomb potential

$$\phi(r) = \frac{qt}{4\pi \epsilon_0 r} \exp(-r/\lambda_{De}). \quad (2.5)$$

The potential distribution around a positive test charge is also known as the Debye-

Hückel or the Yukawa potential.

2.2 Criteria for the plasma state

The Coulomb field of a test particle is screened over a distance of the order of λ_{De} . We stress the following points for the plasma state:

- For a length L much smaller than λ_{De} , the plasma should exhibit quasi neutral behavior, i.e. the net charge density is zero.
- The number of particles in a Debye sphere is $N_D = (4\pi/3)n_{e0}\lambda_{De}^3 \gg 1$. This condition makes sure that the collisional influence is not too large in the plasma, and that the dynamics is dominated by collective forces. In case this condition is not fulfilled, one speaks of "strongly coupled plasmas", which behave quite differently from normal plasmas.

2.3 Physical regimes for classical and quantum plasmas

Plasma physics has vast applications in low-temperature laboratory plasmas (gas discharges), in high energy density plasmas, e.g. for instance Inertial Confinement Fusion (ICF) schemes, in Magnetic Confinement Fusion (MCF) schemes, in magneto-inertial fusion schemes, in our solar system (viz. geospace plasmas, heliospheric plasmas), in planetary systems, and in astrophysical environments (e.g. interstellar medium, the cores of white dwarf stars, magnetars, neutron stars, etc.), and in MHD energy conversion. The plasma fusion efforts will provide a cost effective, limitless and environmentally friendly alternative energy, because the method would not produce unwanted waste fusion products, and in most cases would expose insignificant hazards to mankind. Plasmas are also used for medical treatments and also for improving lamination, printing, and adhesion.

Classical plasma physics is mainly focused on regimes of high temperatures and low densities. Over many years, new emerging subfields of plasma physics have been growing rapidly, such as strongly coupled dusty and quantum plasmas, ultra-cold neutral plasmas, and intense laser-plasma/solid density plasma interactions. In the next section, we will briefly characterize certain physical parameters for quantum-dusty plasmas and their applications, which have been an interest in our research. In paper 6, we have investigated a new purely growing ion streaming instability in a quantum-dusty plasma.

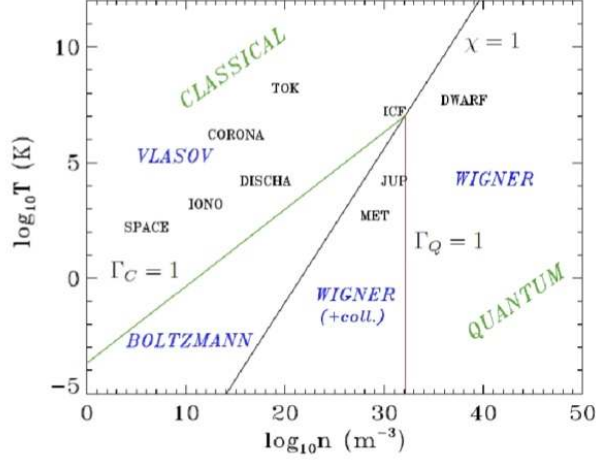


Figure 2.2: Plasma diagram in the $\log T - \log n_0$ plane, separating the quantum and classical regimes. METAL: electrons in a metal; IONO: ionospheric plasma; TOK: plasma in the typical tokamak experiments for nuclear fusion; ICF: inertial confinement fusion; SPACE: interstellar plasma; DWARF: white dwarf star.

2.4 Basic parameters for quantum plasmas

The quantum effects in plasmas become important when the de Broglie length λ_{Be} is similar to the Thomas-Fermi radius $\lambda_{Fe} = V_{Fe}/\omega_{pe}$. The characteristic de Broglie length in a dense plasma with degenerate electrons is given by $\lambda_{Be} = \hbar/m_e V_{Fe}$, where $V_{Fe} = (2k_B T_{Fe}/m_e)^{1/2} = (3\pi n_{e0})^{1/3} \hbar/m_e$ is the Fermi electron speed, $k_B T_{Fe} = E_{Fe}$ is the Fermi electron energy, and \hbar the Plank constant divided by 2π . Naturally, the quantum effects play an important role whenever the plasma temperature T_e is greater than T_{Fe} , whereas a classical plasma description is typically adequate in the opposite limit. The coupling parameter in quantum plasmas reads

$$\Gamma_Q = \left(\frac{\hbar \omega_{pe}}{E_{Fe}} \right)^2 = \left(\frac{1}{n_{e0} \lambda_{Fe}^3} \right)^{2/3}, \quad (2.6)$$

which describes the ratio between the plasmonic energy associated with the electron plasma oscillations and the Fermi electron energy. The characteristic de Broglie length can be expressed in terms of the quantum coupling parameter as $\lambda_{Be} = \sqrt{\Gamma_Q \lambda_{Fe}}$. For $n_{e0} \lambda_{Be}^3 \geq 1$, the quantum effects become important, representing that λ_{Be} is equal to or greater than the average inter-electron distance $d = n_{e0}^{-1/3}$. However, when $\lambda_{Be} \rightarrow \lambda_{De}$, the quantum coupling parameter tends to the classical coupling parameter, i.e. $\Gamma_Q \rightarrow \Gamma_C$. In the classical regime, $\hbar \rightarrow 0$, and the electrons can be considered point-like and no quantum interference effect shows up. Thus, classical and quantum regimes occur in different physical environments [53].

2.5 Quantum dusty plasmas

A quantum dusty plasma consists of degenerate electrons, non-degenerate ions and negatively/positively charged dust particles [54]. Naturally, the electrons are the lightest particles compared to the ions and dust particles, and therefore the quantum degeneracy of electrons is rather important in dense quantum plasmas. Since the ions and dust particles are relatively massive, one can neglect the quantum effects for ions and dust grains. The latter are ubiquitous in the universe, such as in the interstellar medium, in interplanetary space, in molecular clouds, in cometary tails, and in planetary rings etc. About twenty years ago, the existence of the dust-acoustic-wave (DAW) was theoretically predicted in a multi component electron-ion-dust plasma by Rao, Shukla and Yu [55]. In such a wave, the restoring force comes from the pressures of the inertialess electrons and ions, whereas the dust mass provides the inertia to maintain the wave.

A new dust mode, whose frequency strongly depends on the dust charge and the dust number density, has been reported [56] in an unmagnetized quantum dusty plasma. The dispersion properties of several electrostatic and electromagnetic waves [57] are studied including the quantum statistical pressure and quantum electron tunneling or quantum recoil effects.

2.6 Theoretical descriptions of plasmas

A plasma is a collection of many charged particles, which can be described microscopically or macroscopically. In order to describe the dynamics of the plasma particles in the presence of electromagnetic fields in plasmas, one uses some simplified mathematical methods. Depending on the problem, one uses three different models to describe the state of plasmas:

- *A single particle approach*
- *The kinetic theory*
- *The fluid description*

A single particle approach provides a microscopic view of the plasma, where the motion of a single charged particle in the presence of electric and magnetic fields is considered. The single particle approach can be quite cumbersome when one deals with large number of particles. Even more importantly, the self-consistent fields generated by the plasma currents and charges cannot be dealt with in a dynamical situation using this approach. In such a case, the plasma dynamics can be described by means of a statistical approach using the kinetic theory. For some applications, it is easier to use

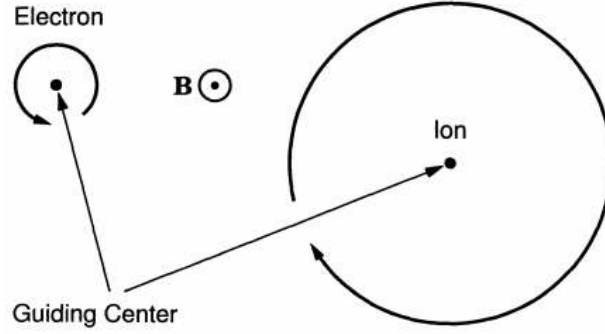


Figure 2.3: *Gyromotion of the electrons and ions in a constant magnetic field*

the fluid description instead of kinetic theory, since the seven independent variables in the latter theory can make both analytical and numerical calculations very challenging. In the next section, we will briefly describe the three different approaches to treat the plasma particle dynamics under the electromagnetic forces.

2.6.1 Single particle motion

Let us consider the motion of a single charged particle in a homogeneous static magnetic field without the electric field. The equation of motion of a charged particle is given by

$$\frac{d\mathbf{v}_j}{dt} = \frac{q_j}{m_j} \mathbf{v}_j \times \mathbf{B}, \quad (2.7)$$

which reveals a circular orbit of a charged particle with the angular gyrofrequency

$$\omega_c = \frac{q_j B}{m_j}, \quad (2.8)$$

where the magnetic field $\mathbf{B} = \hat{z}B$ is along the z -axis in a Cartesian coordinate system.

We note that ω_c depends on the charge and mass of the plasma particles. The ions would gyrate in the left-handed sense and the electrons in the right-handed sense (see, Fig. 2.3). Since the ions (in case of protons) are 1836 times heavier than the electrons, the ions would gyrate much more slower than the electrons. In this case, the particles would gyrate in a circular orbit across the external magnetic field with a constant velocity. The gyroradius is given by

$$r_L = \frac{v_{\perp}}{\omega_c}, \quad (2.9)$$

where the velocity $v_{\perp} = \sqrt{v_x^2 + v_y^2}$ is perpendicular to the external magnetic field. If

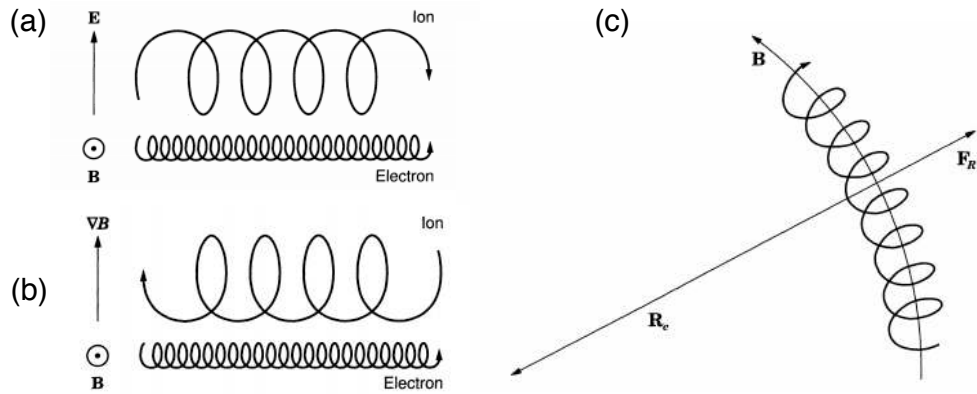


Figure 2.4: (a) Particle drifts in the crossed electric and magnetic fields (b) Particle drifts due to a magnetic field gradient (c) Curvature drift along curved field lines.

we next consider a constant electric field \mathbf{E} , in addition to the magnetic field, we will find that the gyrating motion is combined with a drift of the guiding center, given by

$$\mathbf{v} = \frac{\mathbf{E} \times \mathbf{B}}{B^2}, \quad (2.10)$$

which is perpendicular to both \mathbf{E} and \mathbf{B} fields, and is independent of the charge and mass of the plasma particles. This is called the $\mathbf{E} \times \mathbf{B}$ drift. Note that the above result breaks down in case the magnetic field is small such that the $\mathbf{E} \times \mathbf{B}$ -drift becomes relativistic. In general, the responses of charged particles with different configurations of the electric and magnetic fields results in different drifts of charged particles, for instance, the polarization drift, the curvature drift, the Grad- \mathbf{B} drift etc., see Fig. 2.4. A necessary condition for describing the particle motion is that the inhomogeneity scale length of the fields is much longer than the Larmor radius, and also that the field changes slowly in time compared to the gyroperiod.

As is well-known, the quantum effects could be included by replacing the Newton equation of motion with the single particle Schrödinger equation in given fields. In physical terms, this will lead to the dispersive spread of an initially well localized wave packet. However, the evolution of the expectation value of the position and momentum is still given correctly by the classical equation of motions, as is ensured by the Ehrenfests theorem. We will return to the effect of quantum particle dispersion when studying the fluid equation of motion in section 2.6.3.

Computing the motion of all plasma particles in plasmas is quite tedious, and not possible in practice. However, one often uses statistical approaches of the plasma dynamics since they are quite useful for many applications. Hence, we need another tool to define the plasma dynamics statistically. The Kinetic theory will be discussed

in the next section for the statistical approach of plasmas.

2.6.2 Kinetic Model

In an equilibrium plasma, the trajectory of an individual particle is quite complicated. Instead of providing a detailed description of the plasma particles, it is rather simple to provide the average description of a large number of plasma particles due to their collective behavior in plasmas. It can be achieved by using a kinetic theory where a single distribution function $f_j(\mathbf{r}, \mathbf{v}, t)$ can be used to define the dynamics of all identical particles. The distribution function is defined by the number of particles per cm^3 at position $\mathbf{r} = x\hat{i} + y\hat{j} + z\hat{k}$ and time t , with velocity $\mathbf{v} = v_x\hat{i} + v_y\hat{j} + v_z\hat{k}$ in a small volume dV of six-dimensional phase space. The number density of the plasma particles is therefore

$$n(\mathbf{r}, t) = \int f_j(\mathbf{r}, \mathbf{v}, t) d^3v. \quad (2.11)$$

The time evolution of the distribution function in a collisionless plasma is determined by the Vlasov equation, which follows from the conservation of phase space density along the particle trajectory. The Vlasov equation reads

$$\frac{\partial f_j}{\partial t} + \mathbf{v}_j \cdot \nabla f_j + q_j (\mathbf{E} + \mathbf{v}_j \times \mathbf{B}) \cdot \nabla_{\mathbf{p}} f_j = 0, \quad (2.12)$$

where q_j , \mathbf{v}_j and f_j are the charge, perturbed velocity, and normalized distribution function associated with the j th component of the plasma species. For the case of non-relativistic velocities, the momentum derivative in Eq. (2.12) can be replaced by $\nabla_p = (1/m)\nabla_v$. In relativistic regime Eq. (2.12) must be used as it stands, and we should consider the distribution function to be a function of momentum i.e $f = f(\mathbf{r}, \mathbf{p}, t)$. In this case, Eq. (2.11) is replaced by $n(r, t) = \int f(\mathbf{r}, \mathbf{p}, t) d^3p$, and the velocity in (2.12) as well as (2.18) is expressed as $\mathbf{v} = \mathbf{p}/\gamma m$, where m is the invariant mass and $\gamma = \sqrt{1 + p^2/m^2c^2}$.

The electric and magnetic fields in plasmas can be determined by using Maxwell's equations. We can also use Ampère's law (when the displacement current in the Maxwell equation is neglected) and Faraday's laws in order to compute the electric and magnetic fields in plasmas. The Maxwell equation is

$$\nabla \times \mathbf{B} = \mu_0 \mathbf{J} + \mu_0 \epsilon_0 \frac{\partial \mathbf{E}}{\partial t}, \quad (2.13)$$

and Faraday's law reads

$$\nabla \times \mathbf{E} = -\frac{\partial \mathbf{B}}{\partial t}. \quad (2.14)$$

The Poisson equation is

$$\nabla \cdot \mathbf{E} = \frac{\rho}{\epsilon_0}. \quad (2.15)$$

The condition

$$\nabla \cdot \mathbf{B} = 0. \quad (2.16)$$

is required in general.

In the non-relativistic kinetic theory, the charge and current densities in plasmas are given by

$$\rho = \sum_j q_j n_j = \sum_j q_j \int f_j d^3v, \quad (2.17)$$

and

$$\mathbf{J} = \sum_j q_j n_j \mathbf{V}_j \equiv \sum_j q_j \int f_j \mathbf{v} d^3v. \quad (2.18)$$

The kinetic theory provides detailed information about plasma species, but mathematically it can be hard to solve in many cases. In many applications, where the plasma is considered as two interpenetrating charged fluids, as the electron and ion fluids, the discrete particle aspect of the plasma can be neglected and the plasma can be treated as a macroscopic fluid, i.e. only the macroscopic parameters (e.g. the density, the fluid velocity, the pressure) are relevant. In the case of a single fluid description, the main physical quantities are referred to as the mean mass velocity and then summed over all species to characterize the entire fluid. The advantage of the fluid model is that it is composed of the evolution equations for a set of physical quantities in time, and three spatial dimensions. But the disadvantage in using the fluid model is that it does not provide information regarding the wave-particle interactions, such as Landau damping. Nevertheless, it does provide a sufficient description of the charged particles, such as the density, the fluid velocity, the temperature and is useful for describing transport properties of charged particles explicitly, depending on the relative motions of various plasma constituents. In the multi-fluid theory, the ions and electrons are described separately. In the next section, we present the equations that are suitable for the fluid approach to treat the plasma wave dynamics.

2.6.3 The fluid model

The first standard assumption in the non-relativistic fluid approach is that free particles cannot be destroyed nor created. This applies if we can neglect re-combination and ionization effects. Such an assumption results in the continuity equation, which can be derived from the zeroth velocity moment of the Vlasov equation, and is

$$\frac{\partial n_j}{\partial t} + \nabla \cdot (n_j \mathbf{v}_j) = 0. \quad (2.19)$$

Next, we note that the plasma fluid will experience pressure and electromagnetic forces. Here, we can obtain an appropriate evolution equation from the Vlasov equation, by multiplying it with $m\mathbf{v}$ and integrating over velocity space. We then obtain the non-relativistic momentum equation

$$m_j n_j \left[\frac{\partial \mathbf{v}_j}{\partial t} + (\mathbf{v}_j \cdot \nabla) \mathbf{v}_j \right] = q_j n_j (\vec{E} + \vec{v}_j \times \vec{B}) - \nabla \cdot \mathbf{P}_j, \quad (2.20)$$

where $\vec{E} + \vec{v}_j \times \vec{B}$ is the electromagnetic force and $\mathbf{P}_j = \int m\mathbf{v}\mathbf{v} f_j d^3v$ is the pressure tensor. Here, we have neglected collisions between the plasma species. Next, an equation for the pressure tensor must be supplied. Here it is common to make rather crude assumptions, and replace the divergence of a pressure tensor with the gradient of a scalar pressure. It is then also standard to consider an ideal gas law with $P = k_B n T$, and let the temperature be described by an adiabatic equation of state with T proportional to n^γ , where γ is the ratio of specific heats. For low-frequency wave phenomena, such that the particles have time to thermalize, it is also common to assume an isothermal equation of state with a constant temperature. The Poisson-Maxwell equations are finally used to close the continuity and momentum equations.

The collisionless fluid equations are valid if the electron-ion collision frequency is much smaller than the electron plasma frequency. Such a situation is common in plasmas in the Earth's magnetosphere, in pulsar magnetospheres, in solar and astrophysical plasmas, etc. The dynamics of heavy ions is important for the low-frequency wave phenomena in plasmas. In magnetized plasmas, one often uses the magnetohydrodynamic (MHD) description of the plasma, which is presented in the next section.

In this thesis, I will be concerned with the non-relativistic quantum hydrodynamic equations that are composed of the continuity equation, the electron momentum equation including the quantum statistical pressure and the quantum recoil force associated with overlapping electron wave functions and electron tunneling through the Bohm potential. Then Eq.(2.20) must be improved. The electron pressure in our Fermi plasma is

$$P_{Fe} = n_e k_B T_{Fe} \quad (2.21)$$

where $T_{Fe} = (3\pi n_e)^{2/3} \hbar^2 / 2m_e k_B$ is the Fermi temperature.

Another basic quantum effect is the dispersive properties of degenerate electrons. This can be incorporated within a fluid model by making a so called Madelung trans-

formation of the Schrödinger equation [58] in which case the quantum equation of motion is transformed into fluid like variables. This leads to the appearance of an effective quantum force added to the right hand side of (2.20), often referred to as the Bohm-de Broglie term, describing the quantum particle dispersive effects. The effective quantum recoil force on electrons reads

$$\mathbf{F}_Q = \frac{\hbar^2}{2m_e} \nabla \frac{\nabla^2(\sqrt{n_e})}{\sqrt{n_e}}. \quad (2.22)$$

Another, slightly more rigorous way to obtain the quantum fluid equations, is to start from the quantum kinetic theory. In particular, the hydrodynamical equations for electrostatic disturbances in an unmagnetized quantum plasma have also been derived by using the Wigner-Poisson (Hartree) model [59],

$$\frac{\partial f}{\partial t} + v \frac{\partial f}{\partial x} + \frac{iem}{2\pi\hbar} \int \int d\lambda dv' e^{im(v-v')\lambda} \times \left[\phi \left(x + \frac{\lambda\hbar}{2} \right) - \phi \left(x - \frac{\lambda\hbar}{2} \right) \right] f(x, v', t) = 0, \quad (2.23)$$

$$\frac{\partial^2 \phi}{\partial x^2} = \frac{e}{\epsilon_0} \left(\int f dv - n_0 \right), \quad (2.24)$$

where $f(x,v,t)$ is the Wigner distribution function $\phi(x,t)$ the electrostatic potential, e and m are the magnitude of the charge and mass of the electrons, respectively. Likewise, as in the classical approach, we integrate Eq. (2.23) over velocity space in order to derive the continuity and momentum equations.

To summarize, the non-relativistic equation of motion in quantum plasmas reads

$$\left(\frac{\partial}{\partial t} + \mathbf{v} \cdot \nabla \right) \mathbf{v} = \frac{q}{m} (\mathbf{E} + \mathbf{u} \times \mathbf{B}) - \frac{\hbar^2 (3\pi)^{2/3}}{2m^2 n} \nabla n^{5/3} + \frac{\hbar^2}{2m^2} \nabla \left(\frac{\nabla^2 \sqrt{n}}{\sqrt{n}} \right). \quad (2.25)$$

Furthermore, the continuity equation and Maxwell's equation remain unchanged. A detailed derivation of the fluid model for a quantum magnetoplasma can be found in Ref. [60]. In that derivation, the electron spin effects have not been included. However, in the case of an ambient magnetic field, the electron-one-half spin dynamics can be important, which has been intensively studied in Refs. [61, 62], where the propagation of spin-dependent soliton structures in pair plasmas have also been considered.

2.6.4 The MHD model

In the magnetohydrodynamic (MHD) description of the plasma, the latter is considered as a single charged fluid in which the plasma particles (viz, electrons and ions) move with the same velocity. The MHD plasma model assumes that the electron gyrofrequency $\omega_{ce} = eB_0/m_e$ is much larger than $2\pi/T$, where T is the characteristic

time-scale of the low-frequency phenomena that one studies.

The advantage of using the single fluid MHD equations, instead of the multi-fluid model, is the simplicity introduced by reducing the number of variables and removing the fast dynamical time-scales. This simplification might be necessary when complicated nonlinear and/or inhomogeneous systems are studied.

Now, let us define the mass density, the mass flow velocity, the current density, and the total pressure for a single plasma fluid. We have

$$\rho \equiv \sum_j m_j n_j = m_e n_e + m_i n_i \equiv n(m_e + m_i) \approx n m_i, \quad (2.26)$$

$$\mathbf{V} = \frac{(n_e m_e \mathbf{v}_e + n_i m_i \mathbf{v}_i)}{\rho_j} \equiv \frac{m_i \mathbf{v}_i + m_e \mathbf{v}_e}{m_i + m_e} \approx \mathbf{v}_i, \quad (2.27)$$

$$\mathbf{j} = \sum_j q_j n_j \mathbf{v}_j \approx n(q_e \mathbf{v}_e + q_i \mathbf{v}_i) \approx n e (\mathbf{v}_i - \mathbf{v}_e), \quad (2.28)$$

and

$$P = P_e + P_i \approx n k_B (T_e + T_i), \quad (2.29)$$

under the quasi neutrality approximation $n_e = n_i = n$, which is valid for low-frequency phenomena in plasmas in which the ion plasma frequency is much larger than the ion gyrofrequency. The temperature T_j is assumed constant.

The single MHD equations in the presence of electric and magnetic fields consist of the mass conservation

$$\frac{\partial \rho}{\partial t} + \nabla \cdot (\rho \mathbf{V}) = 0, \quad (2.30)$$

and the momentum equation

$$\rho \left(\frac{\partial}{\partial t} + \mathbf{V} \cdot \nabla \right) \mathbf{V} = \mathbf{j} \times \mathbf{B} - \nabla P. \quad (2.31)$$

In the MHD description, one also uses Ohm's law

$$\mathbf{E} + \mathbf{V} \times \mathbf{B} = \eta \mathbf{j}, \quad (2.32)$$

where $\eta = m_e \nu_{ei} / n e^2$ is the resistivity, and ν_{ei} the electron-ion collision frequency.

Furthermore, to close the system we need Faraday's law

$$\frac{\partial \mathbf{B}}{\partial t} = -\nabla \times \mathbf{E}, \quad (2.33)$$

and Ampère's law

$$\nabla \times \mathbf{B} = \mu_0 \mathbf{j}, \quad (2.34)$$

which is valid for electromagnetic perturbations with the phase speed much smaller than the speed of light in vacuum. This also corresponds to the neglecting the displacement current in the Maxwell equation. The effect of the charge separation is neglected, since the whole plasma is moving as a single fluid. The $\mathbf{j} \times \mathbf{B}$ force can be obtained by using Eq. (2.34), yielding

$$\mathbf{j} \times \mathbf{B} = \frac{-\nabla B^2}{2\mu_0} + \frac{(\mathbf{B} \cdot \nabla)\mathbf{B}}{\mu_0}, \quad (2.35)$$

where $B^2/2\mu_0$ and $(\mathbf{B} \cdot \nabla)\mathbf{B}/\mu_0$ represent the magnetic pressure and the magnetic tension force, respectively.

In a collisionless MHD plasma, there is no diffusion of the magnetic fields in the plasma, and the magnetic lines of force are just frozen into the plasma. However, in the presence of electron-ion collisions (or turbulent collisions) there appears a finite plasma resistivity which, in combination with sheared magnetic fields, produce tearing mode instabilities via which the magnetic energy is converted into plasma kinetic energy. This phenomena is referred to as magnetic field reconnection. It is relevant for understanding the origin of changes in magnetic field topology (e.g. magnetic islands) and charged particle acceleration in both space and laboratory plasmas [63].

Finally, in non-ideal MHD plasmas, one has to account for the Hall term due to the appearance of the $\mathbf{j} \times \mathbf{B}$ term in the generalized Ohm's law. Here, the phenomena would appear on the ion skin depth (c/ω_{pi}) scale. The Hall-term becomes important and whenever the characteristic scale-lengths are shortened (to approach the ion skin-depth scale), or the frequency is increased (to approach the ion gyrofrequency).

The quantum analog of the classical magnetohydrodynamic equations has been derived by Haas [64], by considering a quantum electron-ion plasma in a strong magnetic field where the degenerate electrons are coupled to the non-degenerate ions through EM forces. The quantum MHD equations are

$$\frac{\partial \rho}{\partial t} + \nabla \cdot (\rho \mathbf{V}) = 0, \quad (2.36)$$

$$\left(\frac{\partial}{\partial t} + \mathbf{V} \cdot \nabla \right) \mathbf{V} = \frac{1}{\rho} \mathbf{j} \times \mathbf{B} - \frac{1}{\rho} \nabla \tilde{P} + \frac{\rho \hbar^2}{2m_e m_i} \nabla \left(\frac{\nabla^2 \sqrt{\rho}}{\sqrt{\rho}} \right) \quad (2.37)$$

Here \tilde{P} is one fluid pressure, defined as

$$\tilde{P} = P\mathbf{I} + \frac{m_e m_i n_e n_i}{\rho m} (v_e - v_i) \otimes (v_e - v_i) \quad (2.38)$$

where $P = P_e + P_i$ and \mathbf{I} is an identity matrix. As usual, an equation of state for the pressure that closes the quantum fluid equations cannot be derived from first principles. Instead a bit of phenomenological modeling is needed. In case the Fermi electron temperature is smaller than the average electron temperature, it is common to consider the degenerate electrons as an isothermal fluid, in which case we have

$$\frac{m_e m_i}{\rho e^2} \frac{D\mathbf{J}}{Dt} - \frac{m_i \nabla \tilde{P}_e}{\rho e} = \mathbf{E} + \mathbf{V} \times \mathbf{B} - \frac{m_i}{\rho e} \mathbf{j} \times \mathbf{B} - \frac{\rho \hbar^2}{2e m_e} \nabla \left(\frac{\nabla^2 \sqrt{\rho}}{\sqrt{\rho}} \right) - \frac{1}{\sigma} \mathbf{j}, \quad (2.39)$$

where $D/Dt = (\partial/\partial t) + \mathbf{v}_e \cdot \nabla$, $\mathbf{J} = \mathbf{j} - n\mathbf{eV}$, $\mathbf{v}_e = \mathbf{V} - (1/en\mu_0)\nabla \times [\mathbf{B}]$, $\sigma = \rho e^2/(m_e m_i \nu_{ei})$ is the longitudinal electrical conductivity. By neglecting slowly varying and small pressures, one can retrieve the complete set of generalized quantum version of the MHD equations

$$\frac{\partial \rho}{\partial t} + \nabla \cdot (\rho \mathbf{V}) = 0, \quad (2.40)$$

$$\left(\frac{\partial}{\partial t} + \mathbf{V} \cdot \nabla \right) \mathbf{V} = \frac{1}{\rho} \mathbf{j} \times \mathbf{B} - \frac{1}{\rho} \nabla \tilde{P} + \frac{\hbar^2}{2m_i m_e} \nabla \left(\frac{\nabla^2 \sqrt{\rho}}{\sqrt{\rho}} \right), \quad (2.41)$$

$$\nabla \tilde{P} = C_s^2 \nabla \rho, \quad (2.42)$$

$$\nabla \times \mathbf{E} = -\frac{\partial \mathbf{B}}{\partial t}, \quad (2.43)$$

$$\nabla \times \mathbf{B} = \mu_0$$

$$\mathbf{j} = \sigma \left[\mathbf{E} + \mathbf{V} \times \mathbf{B} - \frac{m_i}{e\rho} \mathbf{J} \times \mathbf{B} - \frac{\hbar^2}{2m_i m_e} \nabla \left(\frac{\nabla^2 \sqrt{\rho}}{\sqrt{\rho}} \right) \right] \quad (2.45)$$

where the linear and nonlinear electron inertial forces have been neglected, We have here denoted $C_s = (k_B T_{Fe}/m_i)^{1/2}$, $\eta = \sigma^{-1}$ the plasma resistivity, and $\mathbf{J} \times \mathbf{B}$ the Hall term.

The ideal quantum MHD equations for a collisionless quantum magnetoplasma are composed of Eq. (2.40), together with

$$\rho \left(\frac{\partial}{\partial t} + \mathbf{V} \cdot \nabla \right) \mathbf{V} = \frac{1}{\mu_0} (\nabla \times \mathbf{B}) \times \mathbf{B} - \nabla \tilde{P} + \frac{\rho \hbar^2}{2m_i m_e} \nabla \left(\frac{\nabla^2 \sqrt{\rho}}{\sqrt{\rho}} \right), \quad (2.46)$$

and

$$\frac{\partial \mathbf{B}}{\partial t} = \nabla \times (\mathbf{V} \times \mathbf{B}), \quad (2.47)$$

2.7 Conclusion

To summarize this chapter, we began with a brief and intuitive description of basic plasma physics and its limitations. Furthermore, we have provided a brief introduction of quantum plasmas. A comprehensive study of plasma dynamics in electromagnetic fields has been described by analyzing three different approaches for classical and quantum plasmas. These introductory descriptions have been reviewed from different books [64–66]. Both electrostatic and electromagnetic waves are very important in plasma physics, since they provide the understanding of many different eigenmodes at multi-scales in plasmas. The modes of wave propagation can be identified from the appropriate dispersion relations. In the next chapter, we will characterize the propagation of linear waves in plasmas.

Waves in plasmas

The collective behavior of plasmas allows for a large number of different wave modes. The free charges make the plasma electrically conductive, so that it strongly responds to electromagnetic fields. Wave phenomena are ubiquitous in plasmas in which both electrostatic and electromagnetic waves of different frequencies can propagate. For most purposes it is sufficient to describe linear wave phenomena in homogenous plasmas by computing the dispersion relation, where the frequency $\omega(k)$ is associated with the wavenumber k . The phase and group velocities of these waves are defined as

$$\mathbf{v}_{ph} = \frac{\omega(\mathbf{k})}{k} \hat{\mathbf{k}}, \quad (3.1)$$

and

$$\mathbf{v}_g = \frac{\partial \omega}{\partial \mathbf{k}}. \quad (3.2)$$

The phase velocity is directed parallel to \mathbf{k} and gives the direction and speed of the propagation of the wave front or phase $\phi(\mathbf{x}, t) = \mathbf{k} \cdot \mathbf{r} - \omega(\mathbf{k})t$, while the group velocity can point a direction different from the phase velocity which gives the direction of the flow of energy and information contained in the wave.

An introduction to linear wave phenomena in unmagnetized and magnetized plasmas is now presented in the following sections, where the basic concepts for the various types of waves and their dispersion relations are briefly examined.

3.1 Waves in an unmagnetized plasma

A plasma is a complex fluid that supports many plasma wave modes obeying Maxwell's equations. The latter dictate how the electric field \mathbf{E} and the magnetic field \mathbf{B} are related to each other. We have

$$\nabla \times \mathbf{E} = -\frac{\partial \mathbf{B}}{\partial t}, \quad (3.3)$$

and

$$\nabla \times \mathbf{B} = \mu_0 \mathbf{j} + \frac{1}{c^2} \frac{\partial \mathbf{E}}{\partial t}. \quad (3.4)$$

By using Eqs. (3.3) and (3.4), the wave equation for a homogeneous plasma can be written as

$$\nabla \times \nabla \times \mathbf{E} = -\mu_0 \frac{\partial \mathbf{j}}{\partial t} - \frac{1}{c^2} \frac{\partial^2 \mathbf{E}}{\partial t^2}. \quad (3.5)$$

The current density \mathbf{j} is created by the motion of the plasma particles, and reads

$$\mathbf{j} = \rho_\sigma \mathbf{v}_\sigma = \sum_{\sigma=e,i} n_\sigma e_\sigma \mathbf{v}_\sigma. \quad (3.6)$$

The momentum equation is then used to solve for the fluid velocity \mathbf{v}_σ

$$m_\sigma n_\sigma \left(\frac{\partial}{\partial t} + \mathbf{v}_\sigma \cdot \nabla \right) \mathbf{v}_\sigma = n_\sigma q_\sigma (\mathbf{E} + \mathbf{v}_\sigma \times \mathbf{B}). \quad (3.7)$$

Here for simplicity, we have invoked the cold plasma approximation, it is valid for perturbations with phase velocities much larger than the thermal speeds. We have also neglected collisions between the electrons and ions, as well as any quantum effects. For finite amplitude perturbations, the plasma system is a nonlinear medium. It is rather difficult to calculate exact solutions for nonlinear systems. In order to investigate the behavior of normal plasma modes, we generally resort first to small amplitude (linear) perturbations and neglect higher order nonlinear terms (e.g. the nonlinear flux $n_j \mathbf{v}_j$, the nonlinear advection $(\mathbf{v}_\sigma \cdot \nabla) \mathbf{v}_\sigma$, the nonlinear Lorentz force $\mathbf{v}_\sigma \times \mathbf{B}$, etc.) The linear equations are then Fourier transformed in both space and time. Effectively this is equivalent to making a plane wave ansatz, i.e. to assuming that perturbations vary as $\exp(i\mathbf{k} \cdot \mathbf{r} - i\omega t)$, thus reducing the differential equations to algebraic equations according to the substitution of $\partial/\partial t \rightarrow -i\omega$ and $\nabla \rightarrow i\mathbf{k}$. Accordingly, from Eqs. (3.5) and (3.7) we have the wave equation

$$-\mathbf{k}(\mathbf{k} \cdot \mathbf{E}) + k^2 \mathbf{E} = \frac{\omega^2}{c^2} \mathbf{E} - \mu_0 \left(\sum_\sigma \frac{n_\sigma e_\sigma^2}{m_\sigma} \right) \mathbf{E}. \quad (3.8)$$

In plasmas, both electrostatic and electromagnetic waves propagate with oscillating electric and magnetic fields. In the next section, we will examine a few of these waves and the approximations needed to find their dispersion relations.

3.1.1 Electrostatic electron plasma (ESEP) waves in an unmagnetized plasma

The ESEP waves are longitudinal waves, which imply $\nabla \times \mathbf{E} = 0$. Substituting this condition in Eq. (3.8) we have

$$\frac{\omega^2}{c^2} \mathbf{E} = \mu_0 \left(\sum_\sigma \frac{n_\sigma e_\sigma^2}{m_\sigma} \right) \mathbf{E}, \quad (3.9)$$

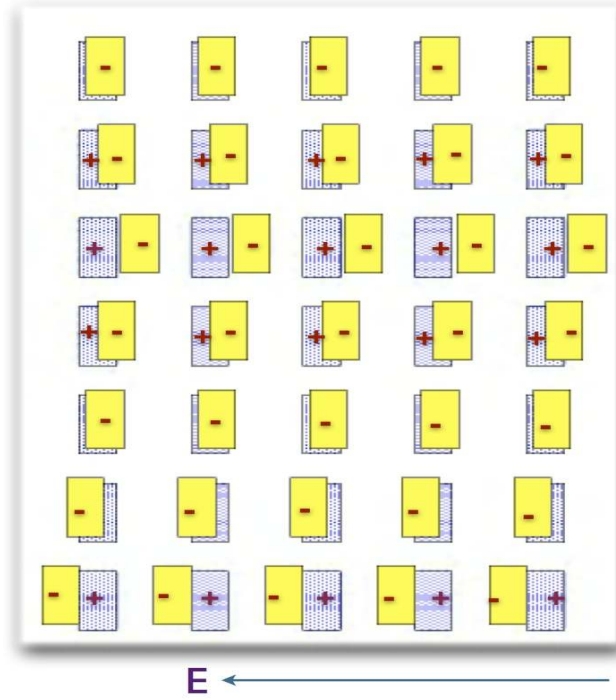


Figure 3.1: *Physical mechanism of electron plasma oscillations: displaced electrons oscillate around fixed ions. (After F. F. Chen, 1974).*

which yields

$$\omega^2 = \frac{1}{\epsilon_0} \left(\sum_{\sigma} \frac{n_{\sigma} e_{\sigma}^2}{m_{\sigma}} \right) = \sum_{\sigma=e,i} \omega_{p\sigma}^2 \quad (3.10)$$

where $\omega = (\omega_{pe}^2 + \omega_{pi}^2)^{1/2}$, which is approximately equal to ω_{pe} , since the ion plasma frequency ω_{pi} is 43 times smaller than the electron plasma frequency for a hydrogen plasma with singly charged ions. The physics of this important oscillation is as follows; If the quasi-neutrality condition is disturbed by some external force, an electric field will be set up due to the charge separation. This electric field will provide a restoring force on the electrons pulling them back to their initial position and hence the electrons will overshoot forth and back around the ions. As a result, a harmonic oscillation appears at the frequency ω that matches the electron plasma frequency

$$\omega_{pe} = \sqrt{\frac{n_e e^2}{\epsilon_0 m_e}} = 5.64 \times 10^4 n_e^{1/2} (\text{rad/sec}). \quad (3.11)$$

The electron plasma wave frequency does not depend on the propagation wave vector \mathbf{k} . Therefore, the group velocity of the electron plasma oscillation is $\mathbf{V}_g = \partial\omega/\partial\mathbf{k} = 0$. Hence, the electrostatic disturbance would not propagate, see Fig. 3.1. This particular kind of plasma wave is referred to as the electron plasma oscillation, carrying only

electron density fluctuations.

In order for the propagating electron plasma oscillations to exist (i.e a non-zero group velocity), we must include the pressure gradient $-\nabla p_e$ in the right-hand side of Eq. (3.7). The effect of a non-zero electron temperature allows the propagation of the dispersive Langmuir wave, which then obeys the dispersion relation

$$\omega^2 = \omega_{pe}^2 + \frac{3}{2} k^2 V_{Te}^2, \quad (3.12)$$

where $V_{Te} = (2k_B T_e / m_e)^{1/2}$ is the electron thermal speed, where the factor 3 comes from the assumption of an adiabatic equation of state for the electrons.

We note that Eq. 3.12 has been derived from the wave equation that results from the combination of the linearized electron continuity and electron momentum equations in which the electron inertial force, the electric force and pressure gradient are retained on equal footings, and Poisson's equation with immobile ions.

In the low-frequency (in comparison with the electron plasma frequency), low-phase velocity (in comparison with the electron thermal speed) electrostatic ion-acoustic waves, inertialess electrons follow the Boltzmann density distribution, $n_e = n_0 \exp(e\phi / k_B T_e)$ that results from the balance between the electric force $n_e e \nabla \phi$ and the pressure gradient $(-k_B T_e \nabla n_e)$, while inertial ions are subjected to the electric force $-e \nabla \phi$ and the pressure gradient, $-3k_B T_i \nabla n_i$, with the ions obeying an adiabatic equation of state. The frequency of the ion-acoustic wave can be obtained from the combination of the Fourier transformed Poisson's equation with the electron density perturbation $n_{e1} \approx n_0 e \phi / k_B T_e$ and an expression for the ion density perturbation n_{i1} that is deduced from the combination of the ion continuity and ion momentum equations. We then have the dispersion relation for the dispersive ion-acoustic wave

$$\omega^2 = 3k^2 V_{Ti}^2 + \frac{k^2 c_s^2}{(1 + k^2 \lambda_{De}^2)}, \quad (3.13)$$

where $V_{Ti} = (k_B T_i / m_i)^{1/2}$ and $c_s = (k_B T_e / m_i)^{1/2}$ are the ion thermal and ion/acoustic speeds, respectively. Equation (3.12) reveals that the dispersion of the ion acoustic wave comes from $n_{e1} \neq n_{i1}$, so that one must consider Poisson's equation for wavelengths comparable to the the electron Debye radius.

The electric field vectors of both Langmuir and ion-acoustic waves are parallel to the propagation wave vectors. The dispersion relation for the Langmuir and ion-acoustic waves are displayed in Fig 3.2.

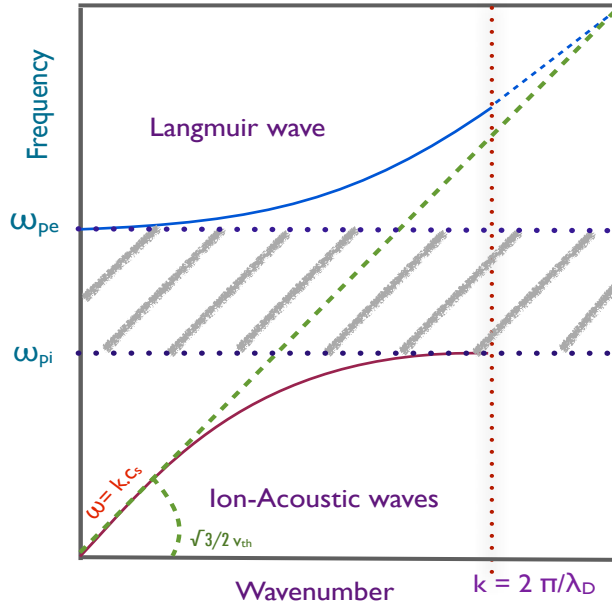


Figure 3.2: Dispersion curves of the Langmuir and ion-acoustic waves.

3.1.2 Electromagnetic (EM) waves in an unmagnetized plasma

The electric and magnetic field vectors of the transverse electromagnetic wave in an unmagnetized plasma are orthogonal to each other and to the direction of the wave propagation. Hence, EM waves satisfy the condition $\nabla \cdot \mathbf{E} = 0$, revealing that there is no density perturbation associated with the wave. The frequency of the EM wave is deduced from the dispersion relation

$$\omega^2 = k^2 c^2 + \omega_{pe}^2, \quad (3.14)$$

which follows from Eq. (3.8).

The group velocity of the EM wave is $\mathbf{V}_g = \partial\omega/\partial\mathbf{k} = c^2\mathbf{k}/\omega$. One observes from (3.14) that for $\omega < \omega_{pe}$ the EM waves have imaginary k , implying that an electromagnetic wave incident onto an overdense plasma will be exponentially damped in the plasma, where the damping length is the of the order of the electron skin depth. In other words, the linear propagation of the EM wave in an unmagnetized plasma is allowed only when $n_e > n_c$, where n_c is the critical density associated with the wave frequency ω , see Fig. 3.3.

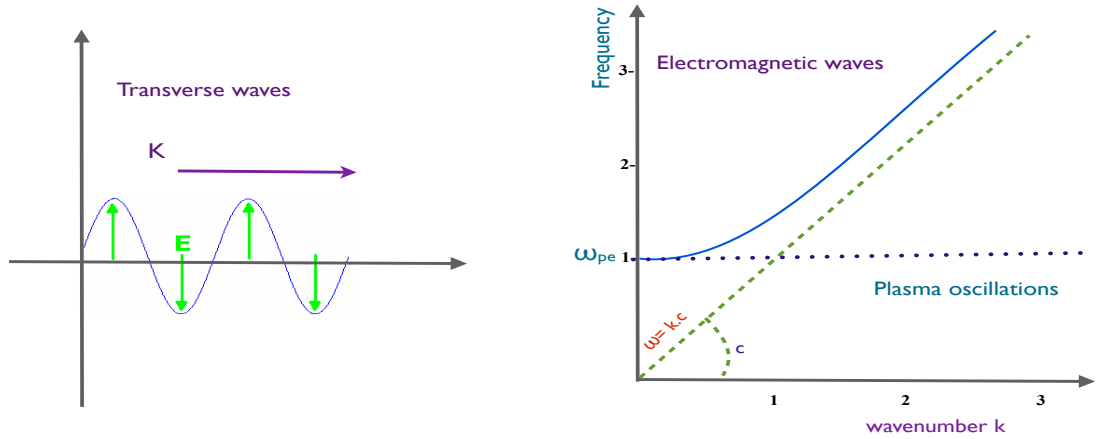


Figure 3.3: Fig. (a) transverse mode; the direction of \mathbf{k} relative to the oscillating electric field \mathbf{E} . Fig. (b) presents dispersion curves for EM waves in an unmagnetized plasma. The dashed line is the vacuum dispersion relation $\omega = kc$.

3.2 Waves in magnetized plasma

In this section, we consider a magnetized plasma with a uniform magnetic field $\hat{\mathbf{z}}B_0$. Specifically, we present the low-frequency hydromagnetic waves by using the MHD theory. For the MHD theory to apply we first note that

$$\left| \frac{\partial}{\partial t} \right| \ll \omega_{ci} = \frac{eB}{m_i}, \quad (3.15)$$

which exhibits the slow wave phenomena in plasma. Furthermore, in the ideal MHD theory, we suppose that $n_i = n_e = n$, and neglect the electron inertial force. We now express

$$\mathbf{v} = \mathbf{v}_0 + \mathbf{v}_1 \equiv \mathbf{v}_1, \quad (3.16)$$

$$\mathbf{B} = \mathbf{B}_0 + \mathbf{B}_1, \quad |B_1| \ll |B_0|, \quad (3.17)$$

$$\rho = \rho_0 + \rho_1, \quad \rho_1 \ll \rho_0, \quad (3.18)$$

and

$$p = p_0 + p_1, \quad p_1 \ll p_0, \quad (3.19)$$

where the subscripts "0" and "1" represent the unperturbed and perturbed quantities, respectively. The equilibrium is assumed to be uniform with $\rho_0 = \text{constant}$, $\mathbf{B}_0 = \text{constant}$, and $p_0 = \text{constant}$. Hence, the linearized ion momentum equation can be written as

$$\rho_0 \frac{\partial \mathbf{v}_1}{\partial t} = \frac{(\nabla \times \mathbf{B}_1) \times \mathbf{B}_0 \hat{\mathbf{z}}}{\mu_0} - V_s^2 \nabla \rho_1, \quad (3.20)$$

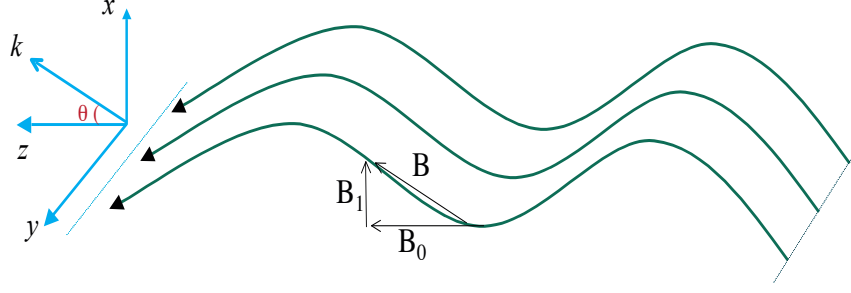


Figure 3.4: Geometry of the wave propagation in a magnetized plasma.

where $V_s = [k_B(T_e + T_i)/m_i]^{1/2}$ is the effective ion-sound speed, and we have assumed an isothermal equation of state for both electrons and ions.

The linearized continuity equation is

$$\frac{\partial \rho_1}{\partial t} + \rho_0 \nabla \cdot \mathbf{v}_1 = 0. \quad (3.21)$$

The linearized momentum and continuity equations are closed by using the linearized Faraday's law

$$\frac{\partial \mathbf{B}_1}{\partial t} = \nabla \times (\mathbf{v}_1 \times B_0 \hat{\mathbf{z}}). \quad (3.22)$$

Supposing that \mathbf{v}_1 , ρ_1 and \mathbf{B}_1 are proportional to $\exp(i\mathbf{k} \cdot \mathbf{r} - i\omega t)$, we can Fourier transform Eqs. (3.20)-(3.22) by letting the operators $\partial/\partial t \rightarrow -i\omega$ and $\nabla \rightarrow i\mathbf{k}$. Without loss of generality, we consider $\mathbf{k} = k_x \hat{\mathbf{x}} + k_z \hat{\mathbf{z}}$ with an arbitrary angle against \mathbf{B}_0 , see fig 3.4. Hence, we have

$$\omega \frac{\rho_1}{\rho_0} = \mathbf{k} \cdot \mathbf{v}_1, \quad (3.23)$$

$$\omega \mathbf{v}_1 = -\frac{B_0 (\mathbf{k} \times \mathbf{B}_1) \times \hat{\mathbf{z}}}{(\mu_0 \rho_0)} + \frac{V_s^2}{\rho_0} \mathbf{k} \rho_1, \quad (3.24)$$

and

$$\omega \mathbf{B}_1 = -B_0 \mathbf{k} \times (\mathbf{v}_1 \times \hat{\mathbf{z}}). \quad (3.25)$$

By using Eqs. (3.21) and (3.23) one can eliminate ρ_1 and \mathbf{B}_1 from Eq. (3.22), obtaining

$$\begin{pmatrix} -\omega^2 + k^2 c_A^2 + k_x^2 V_s^2 & 0 & k_x k_z V_s^2 \\ 0 & -\omega^2 + k_z^2 c_A^2 & 0 \\ k_x k_z V_s^2 & 0 & \omega^2 + k_z^2 V_s^2 \end{pmatrix} \begin{pmatrix} v_x \\ v_y \\ v_z \end{pmatrix} = 0 \quad (3.26)$$

A non-trivial solution of Eq. (3.26) requires that the determinant of the matrix is

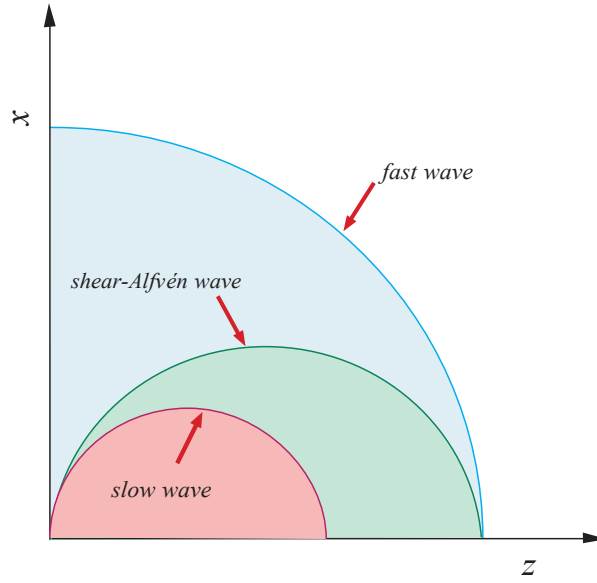


Figure 3.5: Phase velocities of the three MHD waves in the x - z plane. Courtesy to Richard Fitzpatrick

zero, yielding the dispersion relation

$$(\omega^2 - k_z^2 c_A^2)[\omega^4 - \omega^2 k^2 (c_A^2 + V_s^2) + k_z^2 k^2 c_A^2 V_s^2] = 0, \quad (3.27)$$

where $c_A = B_0/(\mu_0 \rho_0)^{1/2}$ is the Alfvén speed. The dispersion relation (3.27) exhibits the shear Alfvén waves, given by $\omega = \pm k_z c_A$, as well as the fast and slow magnetosonic waves, given by $\omega^2 = (\Omega_m^2/2) \pm (1/2)\sqrt{\Omega_m^2 - 4k_z^2 k^2 C_A^2 V_s^2}$, are decoupled (e.g., fig. 3.5). Here, we have denoted $\Omega_m^2 = k^2(c_A^2 + V_s^2)$. The plus (minus) sign refers to the fast (slow) magnetosonic mode.

3.3 Summary

There are a great variety of possible plasma waves in magnetoplasmas that can be easily studied, depending on the direction of the wave vector and the polarization of the EM waves with respect to the background electric and magnetic fields. Examples in a uniform magnetoplasma include the high-frequency ordinary (the electric field vector polarized along the external magnetic field direction) and extraordinary (elliptically polarized waves accompanying finite density perturbations) electromagnetic waves, circularly polarized electromagnetic electron-cyclotron and electron whistlers that propagate obliquely to the external magnetic field direction, fast and slow magneto-sonic waves that are coupled with the low-frequency ion-cyclotron-Alfvén waves, inertial and kinetic Alfvén waves, and many other electrostatic eigen-

modes (e.g. the high-frequency electron Bernstein modes, propagating upper-hybrid waves, low-frequency lower-hybrid and electrostatic ion cyclotron waves, obliquely propagating dispersive ion-acoustic waves, etc.

Various types of waves are useful for heating plasmas and for diagnostics purposes. The free energy accessible to excite instabilities exists in a variety of forms, as for example found in laboratory and space plasmas. Common instabilities that lead to the excitation of numerous wave modes in plasmas include the cross-field current, lower-hybrid-drift, drift kink/sausage, current driven Alfvénic, Kelvin-Helmholtz, tearing, and entropy anti-diffusion instabilities. The free energy sources associated with the deviation from the thermodynamics equilibrium distribution functions could also excite waves. In the present thesis, our main objective is to provide detailed studies of the plasma wave instabilities and the plasma magnetization that occur in different physical environments. In chapter 4, we first critically examine and evaluate several mechanisms that are responsible for the generation of seed magnetic fields in plasmas.

Mechanisms for the plasma magnetization

This chapter is mainly a phenomenological description of different mechanisms for generating magnetic fields in plasmas. The plasma magnetization is attributed to sources that foster motion of the background plasma electrons against the ions. Furthermore, the currents are driven by electric fields, and thus the interplay between electric fields, electron currents and magnetic fields must be understood in a self-consistent framework.

4.1 Motivation

During the last few decades, the generation of magnetic fields has been studied in different areas of physics, such as in cosmic environments (e.g. supernova remnants, gamma-ray bursts), and in laser produced plasmas. Thus, magnetic fields are found to be important in every scale hierarchy of various plasma systems. The usual question posed is: How can an initially magnetic-field free plasma give rise to a non-zero "seed magnetic field"? The answer to this question rests on identifying suitable mechanisms that are responsible for creating the electron current \mathbf{j}_e and the electric field \mathbf{E} that are required for generating the seed magnetic field \mathbf{B} . Neglecting the displacement current in Maxwell's equations, we have

$$\nabla \times \mathbf{B} \approx \mu_0 \mathbf{J} \equiv -\mu_0 e (n_e \mathbf{v}_e - n_i \mathbf{v}_i), \quad (4.1)$$

and

$$\frac{\partial \mathbf{B}}{\partial t} = -\nabla \times \mathbf{E}, \quad (4.2)$$

where the electron and ion fluid velocities, \mathbf{v}_e and \mathbf{v}_i , in turn, are controlled by the electromagnetic fields \mathbf{E} and \mathbf{B} , as well as by the forces involving the gradients of the plasma and electromagnetic wave intensity. Thus, the key issue is how to tear apart the electrons and ions, so that there will be electric fields and currents due to the motion of the electrons against the ions.

It has been shown that the seed magnetic fields in plasmas can be generated by several mechanisms, e. g. due to non-parallel electron density and temperature gradients

$(\nabla n_e \times \nabla T_e)$ (known as the Biermann battery [67]), by electron temperature anisotropy (known as the Weibel instability [68]), by counterstreaming charged particle beams (known as the current- filamentation instability [69]), due to the inverse Faraday effect [70, 71], and by the ponderomotive forces of intense laser beams [72–74]. These mechanisms describe how the motion of electrons generates the space charge electric field and currents that are sources for the seed magnetic fields in plasmas. We will discuss in more detail each of these mechanisms for the magnetic field generation in the following subsections.

4.2 The $\nabla n_e \times \nabla T_e$ (The Biermann battery)

About sixty years ago, Schlütter and Biermann [75] demonstrated in the context of rotating magnetized stars that, in a non-relativistic plasma without equilibrium electron flow, the presence of an electron temperature gradient that is not parallel to the density gradient will give rise to a pressure force $-\nabla P_e$, where the electron pressure is $P_e = k_B n_e T_e$, that will swiftly move the lighter electrons against the heavy ions so that there are both a space charge electron field and electron currents. Neglecting the linear and nonlinear inertia of the electron fluid, the electric field is determined from the non-relativistic electron momentum equation

$$0 = -e(\mathbf{E} + \mathbf{v}_e \times \mathbf{B}) - \frac{k_B T_e \nabla n_e}{n_e} - \frac{k_B n_e \nabla T_e}{n_e}, \quad (4.3)$$

which shows how the electromagnetic forces and the electron pressure gradient balance each other in plasmas.

Now, by using Eq. (4.3) we can eliminate \mathbf{E} from (4.2), obtaining

$$\frac{\partial \mathbf{B}}{\partial t} = \nabla \times (\mathbf{v}_i \times \mathbf{B}) + \frac{1}{\mu_0 e n_e} \nabla \times [\mathbf{B} \times (\nabla \times \mathbf{B})] + \frac{k_B}{e n_e} (\nabla T_e \times \nabla n_e), \quad (4.4)$$

where we have assumed $n_i = n_e$. It follows from Eq. (4.4) that the baroclinic vector (the third term in the right- hand side of (4.4)) is non-zero when the equilibrium electron temperature and density gradients are non-parallel. This baroclinic vector is responsible for the seed magnetic fields. The first and second terms in the right-hand side of (4.4) are associated with the ion flow and the $\mathbf{j} \times \mathbf{B}$ force, respectively. They become important in the long term evolution of the magnetic fields that are spontaneously generated by the non-parallel electron temperature and density gradients. Thus, this mechanism generates a dc magnetic field when there is an angle between the equilibrium density and temperature gradients in plasmas.

In the context of laser-produced plasmas, the baroclinically induced magnetic fields

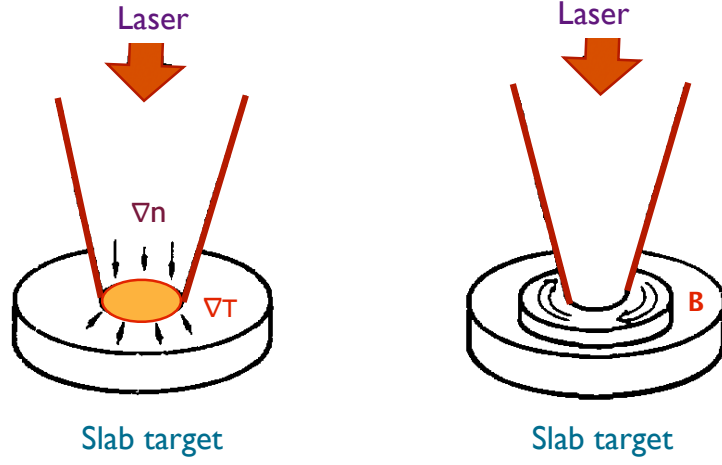


Figure 4.1: Schematic representation of toroidal dc magnetic fields produced by the $\nabla n_e \times \nabla T_e$ mechanism (after Ref. [67]).

were investigated by Stamper et al. [13]. The simplest description of this mechanism is as follows:

For a target irradiated with one finite-sized laser beam, this process is most likely to occur in the outer regions of the laser spot, as shown in Fig. 4.1. The density gradient points into the solid-density target face, whereas near the edge of the laser spot the temperature gradient points radially inward toward the axis of the laser beam. The magnetic field is toroidal in shape, has a scale size comparable to the spot radius, and falls to zero at the axis of the laser beam. Since the intensity distribution of the laser beam is usually rather flat near the middle of the focal spot, radial temperature gradients are thought to be small there. Thus, one expects low magnetic fields at the center of the focal region. The order of magnitude of the magnetic field over a time Δt is roughly $\delta t(m_e/e)(V_{Te}^2/L_n T_T) \sin \theta$, where $V_{Te} = (k_B T_e/m_e)^{1/2}$ is the electron thermal speed, L_n and L_T are the scale lengths of the density and electron temperature gradients, respectively, and θ is the angle between the direction of the density and temperature inhomogeneities.

To estimate the steady-state size of the magnetic field B_s , one could balance the baroclinic driver and the curl of the $\mathbf{u} \times \mathbf{B}$, where $\mathbf{u} = \langle \mathbf{v}_i \rangle$ is the outward average ion fluid velocity, obtained from Eq. (4.4)

$$B_s \simeq \left(\frac{m_e L}{e} \right) \left(\frac{V_{Te}^2}{c_s L_n L_T} \right), \quad (4.5)$$

where L is the scale size of the variation of the $\mathbf{u} \times \mathbf{B}$ flow, $|\mathbf{u}| \sim c_s$, and c_s is the ion sound speed. The angular factors due to the various cross products in Eq. (4.4) are

assumed to be of order unity.

For a 1-KeV hydrogen plasma with the electron temperature and density gradient scale lengths of order $20 \mu m$, one would obtain a magnetic field strength of the order $\simeq 4$ MG at place where the density and temperature gradients were at large angles relative to each other. Recently, huge magnetic fields (of the order of 340 MG) have been measured in the high-density region of plasmas produced during intense laser-matter interactions, near the critical density surface [76].

In cosmological context, non-parallel density and temperature gradients can arise in a number of ways. For example, cosmic ionization fronts are produced when the first ultraviolet photon sources, like star bursting galaxies and quasars, are turned on to ionize the intergalactic medium (IGM); here the temperature gradient is normal to the front. However, a component of the density gradient can arise in a different direction, if the ionization front is sweeping across arbitrarily laid down density fluctuations, which will later collapse to form galaxies and clusters. Such density fluctuations, will in general, have no correlation to the source of the ionizing photons, resulting in a thermally generated electric field which has a curl, and magnetic fields correlated on galactic scales can grow. After compression during galaxy formation, they turn out to have a strength of a few micro-Gauss [77].

Numerical examples for the cosmic plasma parameters [78] reveal that at the temporal-spatial scales of cosmic plasmas, one cannot come up with the seed magnetic fields, deduced from either (4.5), that are of the order of 30 - 100 μG in the Early Universe or in our galaxy [1, 79]. Thus, the mechanism associated with the traditional baroclinic vector or its extension is, unfortunately, not capable of providing a satisfactory answer to the origin of the seed magnetic fields in cosmic plasmas, since it can only act on scales smaller than the galactic scale. Hence, the efficiency of the turbulent galactic dynamo is still being debated.

4.3 The Weibel instability

The Weibel instability [68] is considered to be the most important example of a purely growing electromagnetic mode in an unmagnetized plasma with electron temperature anisotropy. In his classic paper, Weibel found that an anisotropic plasma having a directional dependence of the temperature is unstable against a magnetic field perturbation. Transverse modes are amplified in a collisionless plasma even in the absence of an external magnetic field. The free energy stored in electron temperature anisotropy produces a purely growing magnetic field. The dispersion relation in an unmagnetized plasma has been derived by using a closed set of linearized Vlasov-Maxwell

equations, viz. Eqs. (2.12)-(2.14). We have

$$\omega^2 - k^2 c^2 - \int_0^\infty \int_{-\infty}^\infty \left(\frac{\partial f_0}{\partial v_0} - \frac{v_0 k}{(\omega + kv_z)} \frac{\partial f_0}{\partial v_z} \right) v_0^2 dv_0 dv_z = 0, \quad (4.6)$$

where ω is the angular frequency of the electromagnetic mode, and the wave vector \mathbf{k} is parallel to the z -direction, and $f_0(v) = F(v_0, v_z)$ is an anisotropic distribution functions for the electrons with $v_0^2 = v_x^2 + v_y^2$. Specifically, we have chosen a bi-Maxwellian electron distribution function (an electron temperature anisotropy $(u_0/u_z)^2 - 1 > 0$) of the form

$$f_0 = \frac{n_0}{v_0^2 u_z (2\pi)^{3/2}} \exp\left(-\frac{v_0^2}{2u_0^2} - \frac{v_z^2}{2u_z^2}\right), \quad (4.7)$$

where u_0 and u_z are the unperturbed thermal velocities corresponding to v_0 and v_z , respectively. In the limit $\omega/kv_z \gg 1$, Eq.(4.6) reads

$$\omega^4 - (\omega^2 + k^2 c^2)\omega^2 - k^2 u_0^2 \omega_{pe}^2 = 0. \quad (4.8)$$

The solution of Eq. 4.8 is

$$\omega = \pm \left(\frac{1}{2} [(\omega_{pe}^2 + k^2 c^2) \pm ((\omega_{pe}^2 + k^2 c^2)^2 + 4k^2 u_0 \omega_{pe}^2)^{1/2}] \right)^{1/2}. \quad (4.9)$$

The negative imaginary solution of Eq. (4.9) shows the growth rate of self-excited magnetic fields. Using $ku_z/\omega \ll 1$ and $u_0 \gg u_z$ we can simplify the expression for the growth rate Γ , obtaining

$$\Gamma = \text{Im}(\omega) = \frac{ku_0 \omega_{pe}}{(\omega_{pe}^2 + k^2 c^2)^{1/2}}, \quad (4.10)$$

which is valid only for $ku_z/\omega \ll 1$. The latter implies that $u_0 \gg u_z$. Hence, a large electron temperature anisotropy is required for instability.

The physical picture of the Weibel instability in the presence of counterstreaming electron beams in plasmas was interpreted by Fried [80]. To understand the physical mechanism of the Weibel instability, Fried studied the anisotropy for electrons and assumed immobile ions in an electron-ion plasma. Due to their anisotropic temperatures, the electrons are moving with the thermal velocity $\mathbf{v} = \pm a\hat{\mathbf{x}}$ along the x -direction (see Fig. 4.2). The anisotropic electron distribution function is given by

$$f_0(v) = \delta(v_x^2 - a^2)\delta(v_y)\delta(v_z). \quad (4.11)$$

Now, let us assume some initial perturbation in the magnetic field $\mathbf{B} = \hat{\mathbf{z}}B_z \cos(ky)$,

which is polarized along the z -axis and propagating along the y -axis, arising from noise. The electrons will be deflected by the magnetic field and will acquire in time an additional z -component of velocity $\delta v_z = \delta t \omega_L a$, where $\omega_L = eB_1/m_e$ is the electron gyrofrequency associated with the oscillating magnetic field. The latter would grow at a rate $\Gamma = \omega_{pe}a/c$. Since the magnetic field changes in time, it generates an electric field perpendicular to the magnetic field $E_x = (\omega/k)B_z$ (assuming $\exp(-i\omega t)$ time dependence), due to Faraday's law. By incorporating these effects, Fried obtained a similar quadratic dispersion relation for ω^2 , as Weibel found,

$$\omega^4 - (k^2 + \omega^2) - k^2 a^2 \omega_{pe}^4 = 0. \quad (4.12)$$

Now, we can allow the thermal velocities to be also in the y and z directions by considering $f_0(v) = \delta(v_x^2 - a_1^2)\delta(v_y^2 - a_2^2)\delta(v_z^2 - a_2^2)$. The net effect is simply to replace a^2 with $a_2^2 - a_1^2$ in Eq. 4.12. The instability could occur only when $a_2 > a_1$. But, if $a_2 = a_1$, unstable modes would no longer occur and one would have a stable electromagnetic wave propagating in an unmagnetized plasma.

The Weibel instability has a wide range of applicability in astrophysical plasmas, such as gamma ray burst sources, supernovae and galactic cosmic environments. Medvedev and Loeb [39] suggested that the Weibel instability is capable of generating a strong small-scale magnetic field in an initially unmagnetized plasma, arising from electron temperature anisotropy. The Weibel instability has been extensively studied in both non-relativistic and relativistic regimes. The case of the Weibel instability with ultra-relativistic electron streams (viz., $v_e/c \sim 1$) has been investigated by Yoon and Davidson [81, 82], who obtained the maximum growth rate

$$\Gamma = \frac{\omega_{pe}}{\gamma^{1/2}}, \quad (4.13)$$

where $\gamma = (1 - v_{e0}^2/c^2)^{-1/2}$ is the relativistic gamma factor, and v_{e0} the electron streaming velocity.

In closing, it should be mentioned that we have not here discussed the generation of magnetic fields and filamentation instabilities due to colliding electron clouds, since the free-energy sources in colliding electron clouds could also drive purely growing magnetic fields. The latter could be saturated when the e-folding time is comparable to the electron gyroperiod in the excited magnetic fields. The saturated magnetic fields, in turn, can be associated with the observed magnetic fields in cosmic and laboratory plasmas.

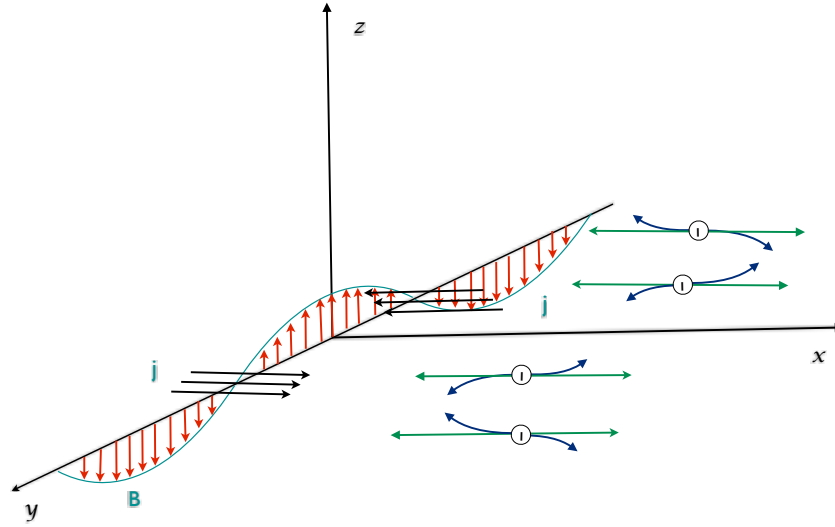


Figure 4.2: *Physical mechanism of the Weibel instability: counter-propagation of two electron beams.*

4.4 Plasma magnetization by a nonuniform electromagnetic beam

The ponderomotive force of a nonuniform intense electromagnetic beam has been considered as a possible alternative mechanism for generating magnetic fields in an unmagnetized plasma [74].

The ponderomotive force is the technical term for the radiation pressure that is exerted by intense laser beams or high-frequency electromagnetic (HF-EM) waves that are interacting with the plasma. In the presence of the HF-EM waves, electrons experience a jitter motion. The advection of the electron fluid and the nonlinear Lorentz force in the electric and magnetic fields of the HF-EM waves give rise to a low-frequency ponderomotive force that primarily acts on the electrons. The ponderomotive force, which is proportional to the HF-EM wave intensity, will swiftly expel the electrons from the region of the high-field intensity such that they instead pile up in the regions of low field intensity.

Let us consider the single particle motion in a given electromagnetic field in the plasma. We assume a monochromatic electromagnetic field given by

$$\mathbf{E}_w(\mathbf{r}, t) = \mathbf{E}_0(\mathbf{r}, t) \cos(\omega t), \quad (4.14)$$

$$\frac{\partial \mathbf{B}_w(\mathbf{r}, t)}{\partial t} = -\nabla \times \mathbf{E}_w(\mathbf{r}, t), \quad (4.15)$$

or

$$\mathbf{B}_w(\mathbf{r}, t) = -\frac{1}{\omega} \nabla \times \mathbf{E}_0(\mathbf{r}) \sin(\omega t) = \mathbf{B}_w(r) \sin(\omega t), \quad (4.16)$$

where \mathbf{E}_0 is the space dependent part of the electric field and $\omega = (k_0^2 c^2 + \omega_{pe}^2)^{1/2}$ is the angular frequency of the HF-EM waves in the plasma. The equation of motion for an electron moving in the HF-EM fields is

$$m_e \frac{d\mathbf{v}_e}{dt} = -e [\mathbf{E}_0(\mathbf{r}, t) \cos(\omega t) + \mathbf{v}_e \times \mathbf{B}_w \sin(\omega t)]. \quad (4.17)$$

In the weakly nonlinear limit, viz. $\mathbf{v}_e/c \ll 1$, (the term $\mathbf{v}_e \times \mathbf{B}_w$ is smaller than the \mathbf{E}_w term. Therefore due to the first order $\mathbf{v}_e = \mathbf{v}_1$, $\mathbf{r} = \mathbf{r}_1$) electrons would oscillate in the direction of \mathbf{E}_w , and in this case one has to solve

$$m_e \frac{d\mathbf{v}_1}{dt} + e\mathbf{E}_0(\mathbf{r}_0, t) = 0, \quad (4.18)$$

$$m_e \frac{d\mathbf{r}_1}{dt} + e\mathbf{E}_0(\mathbf{r}_0, t) \cos(\omega t) = 0, \quad \mathbf{v}_1 = \frac{d\mathbf{r}_1}{dt}. \quad (4.19)$$

The solution of (4.19) is

$$\mathbf{v}_1 = -\frac{e\mathbf{E}_0(\mathbf{r}_0) \sin(\omega t)}{m_e \omega}, \quad \mathbf{r}_1 = \frac{e\mathbf{E}_0(\mathbf{r}_0) \sin(\omega t)}{m_e \omega^2}. \quad (4.20)$$

To study the equations to second order in the amplitude, we write

$$\mathbf{v}_e = \mathbf{v}_1 + \mathbf{v}_2, \quad \mathbf{E}_0 = \mathbf{E}_0(\mathbf{r}_0 + \mathbf{r}_1) \approx \mathbf{E}_0(\mathbf{r}_0) + (\mathbf{r}_1 \cdot \nabla) \mathbf{E}_0(\mathbf{r} = \mathbf{r}_0), \quad \mathbf{B}_w = \mathbf{B}_w(\mathbf{r}_0). \quad (4.21)$$

After substituting Eqs. (4.20) and (4.21) into (4.17), we obtain the second order equation

$$m_e \frac{d\mathbf{v}_2}{dt} = -e [(\mathbf{r}_1 \cdot \nabla) \mathbf{E}_0(\mathbf{r}_0) \cos(\omega t) + \mathbf{v}_1 \times \mathbf{B}_w \sin(\omega t)] \quad (4.22)$$

Substituting Eqs. (4.16) and (4.20) into Eq. (4.22) and averaging over the period $2\pi/\omega$, one can calculate the average nonlinear force

$$\langle \mathbf{F}_{NL} \rangle = m_e \left\langle \frac{d\mathbf{v}_2}{dt} \right\rangle = -\frac{e^2}{2m_e \omega^2} [(\mathbf{E}_0 \cdot \nabla) \mathbf{E}]_0 + \mathbf{E}_0 \times (\nabla \times \mathbf{E}_0). \quad (4.23)$$

In Eq. (4.23), the first term in right-hand side is the force which causes the electrons to move in a linear trajectory and the $\mathbf{E}_w \times \mathbf{B}_w$ force (second term into the right-hand side) acting on the electron and distorts the linear motion into a figure 8 trajectory. By using the identity

$$\mathbf{E}_0 \times (\nabla \times \mathbf{E}_0) = \frac{1}{2} \nabla E_0^2 - (\mathbf{E}_0 \cdot \nabla) \mathbf{E}_0, \quad (4.24)$$

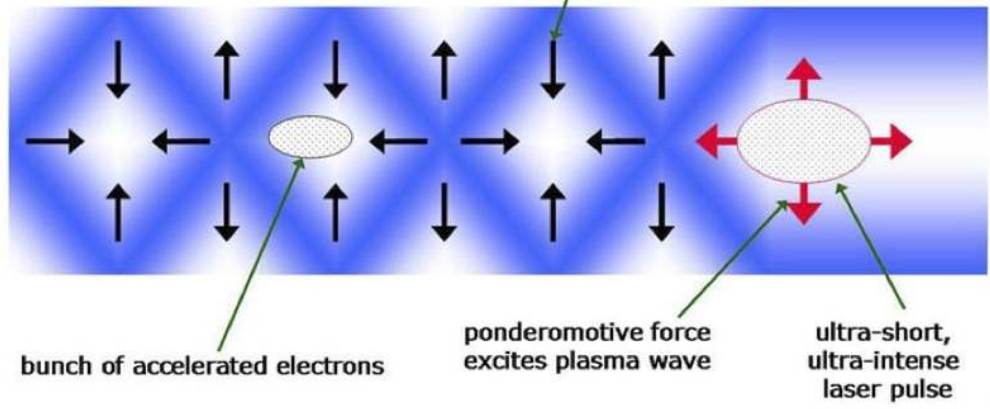


Figure 4.3: The physical mechanism of the ponderomotive force associated with the high-power laser beams (Courtesy to <http://phys.strath.ac.uk/alpha-x/pub/Project/twofa.html>).

and multiplying Eq. (4.23) with the electron number density n_e , one can obtain the ponderomotive force per unit volume for an isotropic collisionless plasma in the presence of a nonuniform HF-EM beam. The result is

$$\mathbf{F}_p = n_e \mathbf{F}_{NL} = \frac{n_e e^2}{4m_e \omega^2} \nabla |\mathbf{E}_0|^2 = -\frac{\omega_p^2}{16\pi\omega^2} \nabla |\mathbf{E}_0|^2. \quad (4.25)$$

The ponderomotive force \mathbf{F}_p is an important source of nonlinearity, which has important consequences for many nonlinear phenomena, such as stimulated scattering instabilities of EM waves, and the plasma magnetization by a nonuniform EM beam. The figure 4.3 depicts the physical mechanism of the EM ponderomotive force.

From the balance between the ponderomotive force of the EM waves, as well as the electrostatic and Lorentz forces on the electrons, we have in the steady state

$$\frac{e^2}{2m_e \omega^2} \nabla |\mathbf{E}_0|^2 = -e (\mathbf{E}_s + \mathbf{u}_{es} \times \mathbf{B}_s), \quad (4.26)$$

where we have assumed that the EM wave ponderomotive force is much stronger than the electron pressure gradient. The electric and magnetic fields associated with the slow plasma motion are denoted by \mathbf{E}_s and \mathbf{B}_s , respectively.

The electrons are coupled to the ions by the slowly varying electric field \mathbf{E}_s . Thus, eliminating the electric field by using $\mathbf{E}_s = -\mathbf{u}_{is} \times \mathbf{B}_s$, where u_{is} is the ion fluid velocity, as well as $\hat{\mathbf{z}} \cdot (\nabla \times \mathbf{B}_s) = \mu_0 \mathbf{j}_s$, we readily obtain [74] from the radial component of Eq. (4.26)

$$\frac{\Omega}{\omega_{pe}} = \frac{e}{m_e \omega r c} \left(-\int_0^r dr_1 r_1^2 \frac{\partial |\mathbf{E}_0|^2}{\partial r_1} \right)^{1/2}, \quad (4.27)$$

where $\Omega = eB_\theta/m_e$ and B_θ is the azimuthal component of \mathbf{B}_s .

Considering an electromagnetic beam with the Gaussian intensity distribution, i. e. $|\mathbf{E}_0|^2 = W_0^2 \exp(-r^2/r_0^2)$, where r_0 is the effective beam radius, we have [74] from Eq. (4.27)

$$\frac{\Omega}{\omega_{pe}} = \frac{r_0 e W_0}{m_e \omega r c} \left[1 - \left(1 + \frac{r^2}{r_0^2} \right) \exp(-r^2/r_0^2) \right]^{1/2}. \quad (4.28)$$

The generated magnetic field is thus proportional to r for $r \ll r_0$ and to r^{-1} for $r \gg r_0$, whereas in the region $r \approx r_0$, Ω is of the order of $\omega_{pe} e W_0 / m_e \omega c$. It turns out that for $e W_0 / m_e \omega c \sim 0.1$, Eq. (4.28) yields $\Omega \sim \omega_{pe}$ at $r = r_0$. Thus, the magnitude of B_θ is of the order of 320 mega-Gauss for a plasma with $n_0 \approx 10^{20} \text{ cm}^{-3}$.

4.5 Summary and conclusion

Summing up, we have here presented a review of possible mechanisms for generating seed magnetic fields in plasmas. Especially, we have described the physics of the baroclinic vector, the Weibel instability, and the ponderomotive force of nonuniform intense electromagnetic beams as sources for the seed magnetic fields in plasmas. Each mechanism has the potential of generating both non-stationary and stationary magnetic fields, the strength of which critically depends on the plasma conditions (e.g. the electron temperature and density gradients and the intensity of the electromagnetic beams). In conclusion, we note that the seed magnetic fields could scatter high energy photons and affect the propagation of EM beams, as well as the cross-field transport of charged particles in plasmas.

In the next section, we will summarize the results of the papers which are included in this thesis. Some elaborate mechanisms have been proposed during my Ph. D. work to amplify the seed magnetic fields into MG fields which was based on known mechanisms, such as non-parallel density and temperature gradients, electron-temperature anisotropy known as the Weibel instability, the ponderomotive forces of nonuniform laser beam and counterstreaming electron-positron beams. Subsequently, the mechanisms lead to important results, such as being responsible for the origin of previously un-explained magnetic fields in galaxy clusters. It is deduced that magnetic fields could have played a significant role in the formation of large scale structures in our universe.

Summaries of the papers

Paper I: Generation of magnetic field fluctuations in relativistic electron-positron (e-p) magnetoplasmas

In this paper, we have investigated purely growing electromagnetic instabilities in a magnetized e-p plasma that contains equilibrium relativistic e-p flows. For this purpose, a new dispersion relation is derived by using a relativistic two-fluid model and the Maxwell equations. The dispersion relation admits purely growing instabilities of electromagnetic perturbations across the ambient magnetic field direction. The results have relevance for understanding the origin of magnetic field fluctuations in cosmological and laser-produced plasmas.

In this paper, I have contributed with analytical calculations and was partially involved in interpreting the results, in addition to participating in discussions and writing of the paper.

Paper II: A new purely growing instability in a strongly magnetized nonuniform pair plasma

A new dispersion relation for the low-frequency (in comparison with the electron gyrofrequency) electrostatic waves in a nonuniform magnetoplasma with the equilibrium density and magnetic field inhomogeneities is derived. For our purposes, we have used Poisson's equation, as well as the electron and positron continuity equations with the guiding center drifts for the electron and positron fluids. The dispersion relation reveals a purely growing instability in the presence of the equilibrium density and magnetic field gradients. The instability arises because of the inhomogeneous magnetic field induced differential electron and positron density fluctuations, which do not keep in phase with the electrostatic potential arising from the charge separation in our nonuniform magnetized e-p plasmas. The present result should be helpful for understanding the origin of nonthermal purely growing electrostatic waves and the glitches in strongly magnetized nonuniform e-p plasmas, such as those in dense neutron stars, in the Crab Nebula, and in some laboratory experiments.

Analytical calculations have been done under the supervision of the coauthor. I also contributed partially in discussions and writing of the paper.

Paper III: Amplification of magnetic fields by polaritonic flows in quantum pair plasmas.

In this paper, we have investigated a new purely growing instability, which can spontaneously create magnetic fields due to the equilibrium polaritonic flows in quantum electron-positron/hole plasmas. The linear dispersion relation has been derived by using the quantum hydrodynamic equations for the polaritons, the Maxwell equation, and Faraday's law. Spontaneously excited magnetic fields can produce cross-field transport of the polaritons at quantum scales. Thus, we expect that the present results would be relevant for understanding the origin of magnetic fields and the associated polaritonic transport at nanoscales in semiconductors, as well as in dense astrophysical pair plasmas and in forthcoming intense laser-plasma interaction experiments.

Analytical calculations have been done by me under the supervision of the coauthors. I also contributed partially in discussions and in writing of the paper.

Paper IV: Ion streaming instability in a quantum dusty magnetoplasma

In this paper, we have shown that a relative drift between the ions and charged dust particles in a magnetized quantum dusty plasma can produce an oscillatory instability involving a quantum dust acoustic-like wave. The threshold and growth rate of the instability are presented. The knowledge of threshold condition, as well as the growth rate and the real part of the wave frequency, as presented here, is essential for identifying non-thermal electrostatic fluctuations that may originate in dense dusty magnetoplasmas, such as those in semiconductors quantum wells. The dust acoustic wave in a magnetized semiconductor plasma can be used as a diagnostic tool for inferring the dust charge.

In this paper, I have contributed with analytical calculations and have been partially responsible for interpreting the results, in addition to participating in discussions.

Paper V: Magnetization of a warm plasma by the nonstationary ponderomotive force of an electromagnetic wave

An electron-temperature anisotropy in a warm plasma can generate magnetic fields by the non-stationary ponderomotive force of a large-amplitude electromagnetic wave. The non-stationary ponderomotive force of the electromagnetic wave pushes electrons locally and creates slowly varying electric fields and vector potentials. The electron currents and electric fields, in turn, produce magnetic fields. The present mechanism for the magnetic field generation is relevant for intense short laser pulse-plasma inter-

action experiments and also for intense x-ray laser pulses interacting with solid density plasma targets. Specifically, spontaneously generated magnetic fields in a warm plasma can affect the electromagnetic wave propagation and the electron energy transport in inertial confinement fusion schemes.

My contribution in this paper has been to carry out analytical calculations, which were checked by my coauthors. I also contributed in discussions and applications of our work.

Paper VI: Proton-temperature anisotropy driven magnetic fields in plasmas with cold and relativistically hot electrons

In this paper, we complement the physical model to present a dispersion relation for a plane polarized electromagnetic wave in plasmas composed of cold electrons, relativistically hot electrons and bi-Maxwellian protons. The free energy in proton temperature anisotropy drives purely growing electromagnetic modes in our three-component plasma. Proton-anisotropy driven instabilities may saturate when the gyrofrequency in the saturated magnetic fields is comparable to the growth rate of the instabilities. The saturated magnetic field can be associated with a large-scale magnetic field, which may co-exist with cold electrons, relativistically hot electrons, and protons having a bi-Maxwellian proton distribution function. The present results are relevant for explaining the origin of spontaneously generated magnetic fields in laboratory and astrophysical plasmas. Finally, we note that the present investigation can be readily generalized for multi-component plasmas with a relativistic bi-Maxwellian proton distribution function.

My contribution in this paper was to perform analytical calculations and participate in discussions and writing of the paper.

Paper VII: Enhancement in the electromagnetic beam-plasma instability due to ion streaming

In this paper, we have investigated the Weibel instability in counterpropagating electron-ion plasmas with the focus on the ion contribution, considering a realistic mass ratio. A generalized dispersion relation (GDR) is derived from a relativistic theory by assuming an initially anisotropic electron temperature, which is represented by a waterbag distribution in momentum space. The GDR reveals an enhanced growth rate due to the ion response. Two-dimensional particle-in-cell simulations support our theoretical analysis, showing a further amplification of the magnetic field on the ion time-scale. The effect of an initially anisotropic temperature is investigated, showing that the growth rate is monotonously decreased if the transverse spread is increased.

Nevertheless, the presence of mobile ions allows an instability to develop for significantly higher electron temperature anisotropy. Suppression of an oblique mode is also explored by introducing a parallel electron velocity spread.

Two and three-dimensional numerical simulations have been carried out by colliding two electron-positron or electron-ion plasmas with or without temperature anisotropy [83, 84], but the ion dynamics for realistic mass ratios have not been investigated with simulations yet, because of limited computational resources. We have performed two-dimensional (2D) kinetic simulations with the particle-in-cell (PIC) code OSIRIS to probe the features of the Weibel instability of two interpenetrating, initially unmagnetized electron-ion plasma clouds with zero net charge and initial electron temperature anisotropy. We demonstrate the possibility of driving an electromagnetic instability on the ion time-scale, and compare our simulation results with our analytical predictions. In the case of an electron-ion plasma, the Weibel instability is a two stage process. Initially, only the electrons respond to the instability since they are much lighter than the ions. This process shuts down due to a strong electron heating and the quasi-isotropization of the electron distribution function. At this stage, the streaming ions start to respond by generating micro-currents and associated magnetic fields that grow at the expense of the energy stored in the ion flow. As a consequence, the instability is further amplified on ion time-scale.

In this paper, I have done all analytical calculations leading to the generalized dispersion relation. Numerical simulations and interpretation of the results have been partially done by me.

ACKNOWLEDGEMENTS

First of all, I want to give my Sincere thanks to Prof. Gert Brodin. This thesis would not have been possible without the help, support and patience of my respected supervisor Prof. Gert Brodin. Secondly, I took this opportunity to express my deep sense of gratitude towards Prof. Mattias Marklund and Prof. L. Stenflo for their constant support and invaluable guidance. I am also overwhelmed by the hospitality of my supervisor during my visits to Umeå University, Sweden. Thanks is also extend to Jens, Mats, Erik, Anton, Chris, Amol, Martina, Shahid, Waleed and Azhar. I also deeply appreciate Katarina and Lena for their kind help with many official matters.

I would like to thank Prof. Luis O. Silva for providing me constant guidance and financial support during 2007-2010. I offer deep regards to all of those who supported me in any respect during the completion of the project. I would like to acknowledge the financial, academic and technical support of the IST, Lisbon, Portugal and its staff, especially Anabela and Ilda who have been always kind to me. My acknowledgments extend to my colleagues for cooperation and help whenever I needed in the research work specially Fiúza , Fabio, Anne, Gainfranco, Dhananjay and Samuel.

My warm thanks to some of my close friend in Lisbon Vipin, Shiva, Archana, Abhik, Amit, Menu, Eli, Sara, DK, Charlotte, Dhasha, Andrea, Ram, Pedro and Joana with whom I shared my great time.

I want to express my deepest gratitude to my respected teacher Professor Padma Kant Shukla for his invaluable guidance and excellent supervision. He is the some one who stood behind me and gave me their unequivocal support throughout, as always, for which my mere expression of thanks likewise does not suffice. I would also like to extend deepest regards to my aunt Mrs. Ranjana Shukla. Without their support, it would have been impossible to reach this level. I am highly indebted for their support. I also would like give warm regards and love to my brothers Prashant Shukla, Pradhiman Shukla and Pushpesh Shukla with whom I shared my great time in Germany. I am extremely grateful to my uncle Shri Surya Kant Shukla who supported my family in bad and good times.

Last but not the least, my mother Mrs. Kaminee Shukla and late father Dr. Prabha Shankar Shukla have been an inspiration throughout my life. My mother has always supported my dreams and aspirations and, if I do say so myself, I think she did a fine job in raising me. I thank her for all she is, and all she has done for me. I also express my love to my sisters, niece and nephew Rashami and Pushpnajali, Tesa and Manash.

Bibliography

- [1] L. WIDROW. "Origin of galactic and extragalactic magnetic fields". *Rev. Mod. Phys.*, **74**, 775 (2002).
- [2] P.P. KRONBERG. "Intergalactic Magnetic Fields". *Phys. Today*, **55**, 1240 (2002).
- [3] M. TATARAKIS, J. WATTS, F.N. BEG, ET AL. "Laser technology: Measuring huge magnetic fields". *Nature (London)*, **415**, 280 (2002).
- [4] P.P. KRONBERG. "Galaxies and the magnetization of intergalactic space". *Phys. Plasmas*, **10**, 1985 (2003).
- [5] LOUKAS VLAHOS, C. G. TSAGAS AND D. PAPADOPOULOS. "Galaxy Formation and Cosmic-Ray Acceleration in a Magnetized Universe". *Astrophys. J.*, **629**, L9 (2005).
- [6] R. SCHLICKEISER, P.K. SHUKLA. "Cosmological magnetic field generation by the Weibel instability". *Astrophys. J.*, **599**, L57 (2007).
- [7] R. SCHLICKEISER. "On the origin of cosmological magnetic fields by plasma instabilities". *Plasma Phys. Controlled Fusion*, **47**, A 205 (2005).
- [8] A.A. RUZMAIKIN, A.A. SHUKUROV AND D.D. SOKOLO. "Magnetic Fields of Galaxies". *Kluwer, Dordrecht*, **39**, 2422–2427 (1988).
- [9] YA.B. ZELDOVICH, A.A. RUZMAIKIN, AND D.D. SOKOLO. "Magnetic Fields in Astrophysics". *Gordon & Breach, New York*, **88**, 437–440 (1983).
- [10] S. WEINBERG. "Gravitation and Cosmology, Wiley". *Wiley & Sons, New York* (1972).
- [11] J. F. HOLZRICHTER, D. EIMERL, E. V. GEORGE, ET AL. "High power pulsed lasers". *J. of Fusion Energy*, **2**, 1 (1982).
- [12] M. G. HAINES. "Magnetic-field generation in laser fusion and hot-electron transport". *Can. J. Phys.*, **64**, 912 (1972).
- [13] J. A. STAMPER, K. PAPADOPOULOS, R. N. SUDAN, ET. AL. "Spontaneous magnetic fields in laser-produced plasmas". *Phys. Rev. Lett.*, **26**, 1012 (1971).
- [14] THE NATIONAL IGNITION FACILITY PROJECT:. <http://www.llnl.gov/nif/project/>.
- [15] THE HIGH POWER LASER ENERGY RESEARCH FACILITY PROJECT:. <http://www.hiper-laser.org/>.

- [16] J. SCHMITT, J.W. BATES, S. P. OBENSCHAIN ET AL. "Shock Ignition target design for inertial fusion energy". *Phys. Plasmas*, **17**, 042701 (2010).
- [17] R. RAMIS AND J. RAMIREZ. "Indirectly driven target design for fast ignition with proton beams". *Nucl. Fusion*, **44**, 720 (2004).
- [18] B. CANAUD AND M. TEMPORAL. "High-gain shock ignition of direct-drive ICF targets for the Laser Mégajoule". *New J. Phys.*, **12**, 043037 (2010).
- [19] R. B. CAMPBELL, R. KODAMA, T. A. MELHORN, ET AL. "Simulation of heating-compressed fast-ignition cores by Petawatt laser-generated electrons". *Phys. Rev. Lett.*, **94**, 055001 (2005).
- [20] R. KODAMA. "Fast heating scalable to laser fusion ignition". *Nature (London)*, **418**, 933 (2000).
- [21] N J SIRCOMB, R BINGHAM, M SHERLOCK ET AL. "Plasma heating by intense electron beams in fast ignition". *Plasma Phys. Control. Fusion*, **50**, 065005 (2008).
- [22] M. TABAK, J. HAMMER, M. E. GLINSKY, ET AL. "Ignition and high gain with ultra-powerful lasers". *Phys. Plasmas*, **1**, 1626 (1994).
- [23] JEREMY MARTIN HILL, MICHAEL H. KEY, STEPHEN P. HATCHETT AND RICHARD R. FREEMAN. "Beam- Weibel filamentation instability in near-term and fast-ignition experiments". *Phys. Plasmas*, **12**, 082304 (2005).
- [24] M. TZOUFRAS, C REN, F.S TSUNG, J. M. TONGE, ET AL. "Space-Charge Effects in the Current-Filamentation or Weibel Instability". *Phys. Rev. Lett.*, **96**, 105002 (2006).
- [25] T.-Y. B. YANG, J. ARONS, AND A. B. LANGDON. "Evolution of the Weibel instability in relativistically hot electron-positron plasmas". *Phys. Plasmas*, **1**, 3059 (1994).
- [26] M. HONDA, J. MEYER-TER-VEHN, AND A. PUKHOV. "Collective stopping and ion heating in relativistic-electron-beam transport for fast ignition". *Phys. Rev. Lett.*, **85**, 2128 (2000).
- [27] R. J. MASON. "Heating mechanism in short-pulse laser-driven cone targets". *Phys. Rev. Lett.*, **96**, 035001 (2006).
- [28] L. O. SILVA, R. A. FONSECA, J. W. TONGE, ET AL. "On the role of the purely transverse Weibel instability in fast ignitor scenarios". *Phys. Plasmas*, **9**, 2458 (2002).
- [29] M. ROTH, T. E. COWAN, M.H. KEY, ET AL. "Fast Ignition by Intense Laser-Accelerated Proton Beams". *Phys. Rev. Lett.*, **866**, 025005 (2001).
- [30] A. S. SANDHU, A. K. DHARMADHIKARI, P. P. RAJEEV, ET AL. "Laser-generated ultra-short multimegagauss magnetic pulses in plasmas". *Phys. Rev. Lett.*, **89**, 225002 (2002).
- [31] J. WIERSMA & A. ACHTERBERG. "Magnetic field generation in relativistic shocks. An early end of the exponential Weibel instability in electron-proton plasmas". *Astronomy & Astrophysics*, **428**, 365 (2004).
- [32] M. V. MEDVEDEV, M. FIORE, R. A. FONSECA ET AL. "Long-time evolution of magnetic fields in relativistic gamma-ray burst shocks". *Astrophys. J.*, **618**, L75 (2004).

- [33] L. O. SILVA. "Physical Problems (Microphysics) in Relativistic Plasma Flows". *AIP Conf. Proc.*, **856**, 109 (2004).
- [34] M. MEDVEDEV, L. O. SILVA, AND M. KAMIONKOWSKI. "Cluster magnetic fields from large-scale structure and galaxy cluster shocks". *Astrophys. J.*, **642**, L1 (2006).
- [35] R. W. KLEBESADEL, I. B. STRONG, AND R. A. OLSON. "Observation of gamma-ray bursts of cosmic origin". *Astrophys. J.*, **182**, L85 (1973).
- [36] T. PIRAN. "The physics of gamma-ray bursts. Reviews of Modern Physics". *Phys. Rev. E*, **76**, 1143 (2004).
- [37] I. J. KATZ. "Two populations and models of gamma-ray bursts". *Astrophys. J.*, **422**, 248 (1994).
- [38] R. SARI, R. NARAYAN AND T. PIRAN. "Cooling Timescales and Temporal Structure of Gamma-Ray Bursts". *Astrophys. J.*, **473**, 204 (1996).
- [39] M. V. MEDVEDEV AND A. LOEB. "Generation of magnetic fields in the relativistic shock of gamma-ray-burst sources". *Astrophys. J.*, **526**, 697 (1999).
- [40] A. BRET, L. GREMILLET, AND J. C. BELLIDO. "How really transverse is the filamentation instability?" *Phys. Plasmas*, **14**, 032103 (2007).
- [41] R. A. FONSECA, L. O. SILVA, J. TONGE, ET AL. "Three-dimensional particle-in-cell simulations of the Weibel instability in electron-positron plasmas". *IEEE Trans. Plasma Sci.*, **30**, 28 (2002).
- [42] A. STOCKEM, M. E. DIECKMANN AND R. SCHLICKEISER. "PIC simulations of the temperature anisotropy-driven Weibel instability: analysing the perpendicular mode". *Plasma Phys. Control. Fusion*, **52**, 085009 (2010).
- [43] J. T. FREDERIKSEN, C. B. HEDEDAL, T. HAUGBLLE, AND A. NORDLUND. "Magnetic field generation in collisionless shocks; pattern growth and transport". *Astrophys. J.*, **608**, L13 (2004).
- [44] R. SARI AND T. PIRAN. "Cosmological gamma-ray bursts: internal versus external shocks". *Mon. Not. R. astr. Soc.*, **287**, 110 (1997).
- [45] R. A. FONSECA, L. O. SILVA, J. TONGE, ET AL. "Three-dimensional Weibel instability in astrophysical scenarios". *Phys. Plasmas*, **10**, 1979 (2003).
- [46] A. HEWISH, S. J. BELL, J. D. H. PILKINGTON, ET AL. "Observation of a Rapidly Pulsating Radio Source". *Nature (London)*, **217**, 709 (1968).
- [47] A. HEWISH, F. P. SCOTT, AND D. WILLS. "Interplanetary Scintillation of Small Diameter Radio Sources". *Nature (London)*, **203**, 1214 (1964).
- [48] A. A. DA COSTA, A. A. AND F. D. KAHN. "High energy in pulsar magnetospheres". *IEEE Trans. Plasma Sci.*, **199**, 211 (1982).
- [49] E. ASSEO. "Pair plasma in pulsar magnetospheres". *Plasma Phys. Control. Fusion*, **45**, 853 (2003).

- [50] G. P. ZANK AND R. G. GREAVES. "Linear and nonlinear modes in nonrelativistic electron-positron plasmas". *Phys. Rev. E*, **51**, 6079 (1995).
- [51] A. SPITKOVSKY. "Current Models of Pulsar Magnetospheres, in book High energy emission from pulsars". *Springer-Verlag Berlin Heidelberg*, p. eds. N. Rea and D. Torres (2011).
- [52] N. MEYER-VERNET. "Aspects of Debye shielding". *Astrophys. J.*, **61**, 249 (1993).
- [53] D. PINES. "Classical and quantum plasmas". *J. Nucl. Energy (Plasma Phys.)*, **2**, 5–17 (2005).
- [54] F. VERHEEST. "Waves in Space Dusty Plasma". *Kluwer Academic, Dordrecht* (2000).
- [55] N.N. RAO, P.K. SHUKLA AND M.Y. YU. "Dust-acoustic waves in dusty plasmas". *Planet. Space Sci.*, **38**, 543 (1990).
- [56] P. K. SHUKLA AND S. ALI. "Dust acoustic waves in quantum plasmas". *Phys. Plasmas*, **12**, 114502 (2005).
- [57] P.K. SHUKLA AND B. ELIASSON. "Colloquium: Nonlinear collective interactions in quantum plasmas with degenerate electron fluids". *Rev. Mod. Phys.*, **83**, 885 (2011).
- [58] F. HAAS, G. MANFREDI AND M. R. FEIX. "Multistream model for quantum plasmas". *Phys. Rev. E*, **62**, 2763 (2000).
- [59] G. MANFREDI. "How to model the quantum plasmas". *Fields Inst. Commun.*, **46**, 263 (2005).
- [60] F. HAAS. "A magnetohydrodynamic model for quantum plasmas". *Phys. Plasmas*, **12**, 062117 (2005).
- [61] G. BRODIN AND M. MARKLUND. "Spin magnetohydrodynamic". *New J. Phys.*, **9**, 277 (2007).
- [62] M. MARKLUND AND G. BRODIN. "Dynamics of spin 1/2 quantum plasmas". *Phys. Rev. Lett.*, **98**, 025001 (2007).
- [63] E. W. HONES JR. (ED.). "Magnetic Reconnection in Space and Laboratory Plasmas". *Geophys. Monogr. Ser.*, **30**, 386 (1984).
- [64] F. HAAS. "Quantum Plasmas, Springer Verlag, New York". *Springer, New York* (2011).
- [65] F. F. CHEN. "Introduction to plasma physics and controlled fusion, Plasma physics, volume 1". *Plenum Press, second edition*, (1984).
- [66] P K SHUKLA AND A A MAMUN. "Introduction to Dusty Plasma Physics". *Institute of Physics, Bristol* (2002).
- [67] L. BIERMANN. "Über den Ursprung der Magnetfelder auf Sternen und im interstellaren Raum". *Zeitschrift Naturforschung Teil A*, **5A**, 65 (1950).

- [68] E. S. WEIBEL. "Spontaneously growing transverse waves in a plasma due to an anisotropic velocity distribution". *Phys. Rev. Lett.*, **2**, 83 (1959).
- [69] M E DIECKMANN. "Simulation study of the filamentation of counter-streaming beams of the electrons and positrons in plasmas". *Plasma Phys. Control. Fusion*, **51**, 065015 (2009).
- [70] J. DESCHAMPS ET AL. "Inverse Faraday effect in a plasma". *Phys. Rev. Lett.*, **25**, 1330 (1970).
- [71] Z. NAJMUDIN ET AL. "Measurements of the inverse Faraday effect from relativistic laser interactions with an underdense plasma". *Phys. Rev. Lett.*, **87**, 215004 (2001).
- [72] I. V. KARPMAN AND H. WASHIMI. "Two-dimensional self-modulation of a whistler wave propagating along the magnetic field in a plasma". *J. Plasma Phys.*, **18**, 173 (1977).
- [73] B.J. GREEN, P. MULSER. "Ponderomotive forces in the interaction of laser radiation with a plasma". *Phys. Rev. A*, **37**, 319 (2002).
- [74] O. M. GRADOV AND L. STENFLO. "Magnetic-field generation by finite-radius electromagnetic beam". *Phys. Lett.*, **95A**, 233 (1983).
- [75] A. SCHLÖUTER AND L. BIERMANN. "Interstellar Magnetfelder". *Z. Naturforsch A*, **5a**, p237 (1950).
- [76] M. TATARAKIS, A. GOPAL, I. WATT ET AL. "Measurements of ultrastrong magnetic fields during relativistic laser-plasma interactions". *Phys. Plasmas*, **9**, 2244 (2002).
- [77] T. TOTANI. "Galaxy Formation by Galactic Magnetic Fields". **517**, L69 (1999).
- [78] K. SUBRAMANIAN, D. NARASIMHA, AND S. M. CHITRE. "Thermal generation of cosmological seed magnetic fields in ionization fronts". *Mon. Not. Roy. Astr. Soc. Lett.*, **271**, L15 (2004).
- [79] R. M. KULSRUD, R. CEN, J. P. OSTRICKER, ET AL. "The protogalactic origin for cosmic magnetic fields". *Astrophys. J.*, **480**, 481 (1997).
- [80] B. D. FRIED. "Mechanism for instability of transverse plasma waves". *Phys. Plasmas*, **2**, 337 (1959).
- [81] P. H. YOON AND R. C. DAVIDSON. "Exact analytical model of the classical Weibel instability in a relativistic anisotropic plasma". *Phys. Rev. Lett. A*, **35**, 2718 (1992).
- [82] P. H. YOON. "Relativistic Weibel instability". *Phys. Plasmas*, **14**, 024504 (2007).
- [83] R A FONSECA, L. O. SILVA, J. TONGE, ET AL. "Three-dimensional particle-in-cell simulations of the Weibel instability in electron-positron plasmas". *IEEE Trans. Plasma Sci.*, **30**, 28 (2002).
- [84] C. REN, M. TZOUFRAS, F. S. TSUNG ET AL. "Global simulation for laser-driven MeV electrons in fast ignition". *Phys. Rev. Lett.*, **93**, 185004 (2004).